NASA Contractor Report 181741

ICASE REPORT NO. 88-63

ICASE

ALGEBRAIC TURBULENCE MODELS FOR THE COMPUTATION OF TWO-DIMENSIONAL HIGH SPEED FLOWS USING UNSTRUCTURED GRIDS

Philippe Rostand

Contract Nos. NAS1-18107, NAS1-18605
November 1988

INSTITUTE FOR COMPUTER APPLICATIONS IN SCIENCE AND ENGINEERING
NASA Langley Research Center, Hampton, Virginia 23665

Operated by the Universities Space Research Association

National Aeronautics and Space Administration

Langley Research Center
Hampton, Virginia 23665

ALGEBRAIC TURBULENCE MODELS FOR THE COMPUTATION OF TWO-DIMENSIONAL HIGH SPEED FLOWS USING UNSTRUCTURED GRIDS

Philippe Rostand
INRIA - MENUSIN
BP105
78153 Le Chesnay Cedex
FRANCE

ABSTRACT

The incorporation of algebraic turbulence models in a solver for the 2D compressible Navier-Stokes equations using triangular grids is described. A practical way to use the Cebeci Smith model, and to modify it in separated regions, is proposed. The ability of the model to predict high speed, perfect gas boundary layers is investigated from a numerical point of view.

This research was supported by the National Aeronautics and Space Administration under NASA Contract Nos. NAS1-18107 and NAS1-18605 while the author was in residence at the Institute for Computer Applications in Science and Engineering (ICASE), NASA Langley Research Center, Hampton, VA 23665. Additional support was also provided under DRET Contract No. 03407901.

CONTENTS

NOMENCLATURE

C_f skin friction coefficient $\frac{2\tau_w}{\rho_\infty u_\infty^2}$

C_h heat flux coefficient $\frac{2q_w}{\rho_\infty u_\infty^3}$

C_p pressure coefficent $2\frac{p-p_\infty}{\rho_\infty u_\infty^2}$

D deformation tensor $D(\vec{u}) = \nabla\vec{u} + \nabla\vec{u}^t - \frac{2}{3}\nabla\cdot\vec{u}I$

E total energy

I identity operator

k kinetic energy of turbulence

M Mach number

P pressure

Pr Prandtl number $\frac{\mu}{\lambda}$

q heat flux

Re free stream Reynolds number $\frac{\rho_\infty u_\infty}{\mu_\infty}$

Re_θ momentum thickness Reynolds number $\frac{\rho_e u_e \theta}{\mu_e}$

T temperature

$\vec{u}$ velocity vector $\vec{u} = (u, v)$

u component of the velocity tangent to the wall

u_s speed scale

W vector of conserved variables $\begin{pmatrix} \rho \\ \rho u \\ \rho v \\ E \end{pmatrix}$

x coordinate tangent to the wall

y coordinate normal to the wall

α Clauser's constant $\alpha = 0.0168$

δ boundary layer thickness defined by $u/u_e = 0.99$

δ^* displacement thickness $\int_0^\delta (1 - \frac{\rho u}{\rho_e u_e}) dy$

δ_i incompressible displacement thickness $\int_0^\delta (1 - \frac{u}{u_e}) dy$

ε isotropic part of turbulence energy dissipation

λ heat conductivity

μ molecular viscosity

κ Von Karman's constant $\kappa = 0.4$

ν kinematic viscosity $\frac{\mu}{\rho}$

∇ gradient operator

$\nabla\cdot$ divergence operator

ω vorticity

SUBSCRIPTS

b at backflow edge

e at boundary layer edge

i at streamwise position $i\Delta x$

j at crossflow position $j\Delta y$

t turbulent

w at wall

∞ free stream conditions

SUPERSCRIPTS

$'$ fluctuating quantities

$-$ averaged

t transpose

I. INTRODUCTION

Solving numerically the laminar compressible Navier-Stokes equations for practical configurations is now within reach [Ca], [Ch1]. Flows around complete aircrafts, including an impressive high Mach number flow around a shuttle [J1], have been successfully computed. However, the complexity of the configurations of industrial interest make these computations to remain a challenging task, even when using modern supercomputers. The results obtained are for steady and laminar flows and still make full use of the computer capability available. This, together with the concern of affordability, is why cost is the major issue when more realistic physical models are taken into account. Still, it is well-known that most configurations of interest are at least locally turbulent, and that the modelling of this turbulence is critical for the reliability of the computations. Though a both cheap and reasonably accurate turbulent closure model is an unavoidable part of a compressible viscous code.

The study of the second part of the reentry of the European shuttle Hermes prompts interest in high-speed, moderate Reynolds flows. With Mach numbers ranging from 5 to 10, real gas effects can be neglected in a first approximation. The purpose of the study is not to predict the details of the flow, which are probably beyond reach anyway, but to give reasonable estimates (say $\pm 10\%$) of the pressure, friction, and heat transfer, and through those of the flight performances of the shuttle.

An implicit algorithm to solve the 2D (3D) compressible Euler equations on unstructured triangular (tetrahedral) grids has been developed in the recent years [St1, St2]. It is based on a finite volume approximation of the equations in conservation form, using control volumes defined by the medians of the triangle (tetrahedras) surrounding each node, and Osher's flux formula [Os1]. It has been extended to solve the Reynolds averaged Navier-Stokes equations, and showed to be able to compute efficiently and accurately two-dimensional laminar boundary layers [Ro1]. The purpose of this work is to include in it some relevant turbulence model.

Our concern here will be two dimensional compressible boundary layers and compression corners, which are the two relevant simple flows (see Fig. 1). Numerous turbulence models have been proposed to solve these problems, and a review would make a (tough) paper by itself. However, they can be classified by the number of extra P.D.E. they introduce, by the order of the closing relation, and by its linearity, i.e., by whether the model is of the eddy viscosity type or not. Nonlinear models have been shown to be an improvement over liner ones in a number of situations (see e.g., [Sp1]), but they will not be our concern here, since we restrict ourselves to two dimensional situations in this first approach.

The choice is then on the number of PDE one wishes to solve; it is our opinion that

1 and 2 equation models offer no significant improvement over algebraic models for the computations of the near-wall flows which are our concern. Consequently, we will restrict ourselves to algebraic models, in which we may later introduce some streamwise history effect through an explicit relaxation model, patterned after that of Shang and Hankey [Sh1]. For attached flows, the models of Cebeci and Smith [Ce1] and of Baldwin and Lomax [Ba1] have been extensively tested, and shown to perform well in the incompressible, transonic and supersonic regimes [V1,Y1]. The Baldwin and Lomax model has the advantage that it does not require to calculate the boundary layer thickness, and has been widely used and tested. However, for detached or near detachment boundary layers, both the Cebeci-Smith and the Baldwin-Lomax model give erroneous results; this is due to the fact that they both rely on Prandtl's mixing length theory, which is no longer relevant after detachment. In separated regions, we will use another algebraic model, introduced by Goldberg [Go1], which prescribes analytically the values of k and ϵ in a separation bubble.

All these models have been previously used and validated; the point of this paper is double: we first want to show that turbulent flows can be efficiently calculated on unstructured grids, using algebraic models; this is not straightforward because the direction normal to the wall is no longer a coordinate axis, so that nonlocal effects are not easy to compute; the details of the implementation are given in part II. Secondly, we want to investigate how well these algebraic models, which were defined after incompressible theories, and thus ignore density fluctuations, will perform for high speed flows. In part III, we will compute a boundary layer at Mach 7.4, and compare the results with the experiments of Hopkins et al. [Ho1]. No data on hypersonic flows over compression corners is known to the author; however, such a high speed computation part of the Hermes workshop [Ma1], will be performed in part IV.

II. ALGEBRAIC TURBULENCE MODELS AND UNSTRUCTURED GRIDS

Linear algebraic turbulence models describe the Reynolds turbulent stress tensor σ_t as

$$\sigma_t = \mu_t D(u) \tag{2.1}$$

and the turbulent heat flux q_t as

$$q_t = \frac{\mu_t}{Pr_t} \nabla T \tag{2.2}$$

where Pr_t is the turbulent Prandtl number, usually assumed constant, and where μ_t is the eddy viscosity, which is an explicit function of the flow variables W, although this function is usually not local. More precisely,

$$\mu_t(x_0, y_0) = f(W(x_0, y), y \geq 0) \tag{2.3}$$

The value of μ_t at a given point depends of the flow variables at all the points at the same streamwise location.

One of the main advantages of algebraic models, which makes them so popular, is their minimum requirement of computer time and storage. Indeed, when one uses an i, j grid (Fig. 2), the value of the eddy viscosity on the grid, μ_{ij}, can be calculated cheaply since

$$\mu_{ti_0j_0} = f(W_{i_0j}, j \geq 0) \tag{2.4}$$

and, in (2.4), many terms in $\mu_{ti_0j_0}$ are common to all points of same streamwise location, and so can be computed only once for each value of i_0.

Whether these desirable features can be conserved for triangular grids, which can be of type a, but also of type b (Fig. 3), is the question that must be answered.

A triangular grid can be, and usually is, at least locally, not orthogonal to the wall. In our approximation ([Ro1]), the flow variables are linear on each triangle, and consequently, we will look for nodal values of the eddy viscosity. The normals to the wall cannot, as in the rectangular structured case, be approximated by a sequence of nodes. There are two ways to calculate the field of eddy viscosities: the first is, for each node, to draw the normal to the wall passing through this node, to track all the elements it gets through (Fig. 4), and then, using flow variables which are piecewise linear on this normal, compute the eddy viscosity, which is valid only for the considered node, since it is the only node with this streamwise location. This is very expensive, both in storage, since the list of the elements used for each node must be stored, unless it is recalculated at each time step, leading to an enormous cpu cost, and in cpu, since a complete viscosity calculation on a normal must be performed for each node.

The other way, which we will use, is to consider a discrete set of normals, namely the normals to the wall, passing through the middle of the wall edges (Fig. 5), compute and store the elements they get through, together with the barycentric coordinates of the middle of their intersection with each element, and then, at each time step, use that information to compute the eddy viscosity on each normal. For each node, it is then necessary to interpolate the values of the eddy viscosity from the two neighboring normals (Fig. 5).

More precisely, the path, in terms of elements and edges, followed by the normal, is computed through an algorithm first derived for characteristic methods ([Da1]), taking in account all the geometrical possibilities: the normal hitting a node, coinciding with an edge, etc. This is done once, at the beginning of the calculation; the result which consists, for each wall edge, of a list of triangles, and of the barycentric coordinates of the middle of the intersection of the normal with each triangle, is stored. The memory needed for that

is equal to the number of wall edges multiplied by the average length of a normal (which is fixed by an a priori bound to the boundary layer thickness) times one integer, the number of the element, and two reals, the coordinates.

$$Sto1 = \text{Wall Edges} \times \text{Average Normal Length} \times (1I + 2R) \tag{2.5}$$

To be able to efficiently make the interpolation of the eddy viscosities from the normals to the whole mesh, one must also store some geometrical quantities. For each node in the boundary layer, one must store the number of the normal just on its left (say), its distance to this normal, plus one integer and one real to allow positioning on this normal, and one integral and one real to allow positioning on the normal on the right (Fig. 6).

Altogether, the memory needed to sore the interpolation data is 3 integers and 3 reals for each of the nodes in the boundary layer.

$$Sto2 = \text{B.L. Nodes} \times (3I + 3R) \tag{2.6}$$

The global storage needed for the turbulence is

$$Sto = \text{Wall Edges} \times \text{Average Normal Length} \, (1I+2R) + \text{Boundary Layer Nodes} \, (3I+3R) \tag{2.7}$$

For example, a flat plate calculation using 100 nodes on the wall and an average 25 nodes in the boundary layer will require 90 Kbytes of storage for the turbulence data, which is quite reasonable. The generation of this data takes about 40 seconds on a SUN workstation for this case.

Once this data is generated, at each time step, the eddy viscosity is evaluated on the normals. This is now straightforward, since we have a normal represented by a set of points at which the flow properties, including the vorticity, are known; we are brought back to the structured orthogonal case. Then the interpolation is performed, which is also straightforward, since all the needed coefficients are stored. Altogether, the calculation of the eddy viscosity when one uses the Baldwin-Lomax model takes less than 1.5% of the global cpu time for an implicit scheme, and less than 4% for an explicit scheme. The evaluation of the eddy viscosity for the aforementioned case takes about 1.2 seconds on a SUN.

The interpolation procedure described earlier is valid only when the solid body is convex; when its not, a given point of the flowfield is usually considered as influenced by two or more walls, and the influences are proportional to the inverse of the distance to the wall. A similar interpolation can be performed; the only added storage is: one real for each node of the boundary layer, representing the ratio of the influence of the eventual two

relevant walls, and in *sto2*, a boundary layer node must be counted twice if it is influenced by two convex components of the wall. This can be handled in a completely automatic and geometry independent way, which is consistent with the finite element spirit.

Although the geometrical part will be much more complicated, the same thing can be done in three dimensions. Normals are drawn starting from the wall faces, and then a spatial interpolation is performed between these normals.

III. HIGH SPEED ATTACHED BOUNDARY LAYERS

Turbulent boundary layers have been studied quite extensively in the last two decades, and described in much details [Ce1]. Many authors have proposed turbulent closure models to predict these boundary layers; the simpler ones, which will be our concern, are those which suppose the turbulent stress tensor $\overline{-\rho u'v'}$ to be proportional to the deformation tensor D:

$$\overline{-\rho u'v'} = \sigma_t = \mu_t D(u) \tag{3.1}$$

where μ_t is the eddy viscosity, which in algebraic models is a function of the flowfield.

Many eddy viscosity laws $\mu_t = \mu_t(W)$ have been proposed through the years, the successful ones separate the boundary layer in an inner and an outer part, which behave differently. In the inner part, the main feature of the analysis is Prandtl's mixing length theory, which predicts the eddy viscosity to be

$$\mu_t = \rho \ell^2 |\omega| \tag{3.2}$$

where $|\omega|$ is the magnitude of the vorticity and ℓ the mixing length. According to Prandtl's theory, in the fully turbulent regime, ℓ is proportional to the distance to the wall:

$$\ell = \kappa y \tag{3.3}$$

To account for the laminar sublayer, this expression has to be modified in the near wall region, as we will see later on.

In the outer part of the boundary layer, it is generally admitted that the eddy viscosity is almost constant, although different values of this constant have been proposed. Cebeci and Smith [Ce1] suppose that

$$\mu_t = \alpha u_e \delta_i \tag{3.4}$$

where α is Clauser's constant, u_e the speed at the edge of the boundary layer, and δ_i the incompressible displacement thickness. Again, this expression must be modified when approaching the edge of the boundary layer to account for the relaminarization of the flow.

From these ideas, Cebeci and Smith proposed an eddy viscosity model defined as:

$$\left.\begin{aligned} &\mu_t = \rho \ell^2 |\omega| \\ &\ell = \kappa y (1 - \exp(-y/A)) \\ &\text{for } y \leq y_c \end{aligned}\right\} \tag{3.4}$$

and

$$\left.\begin{aligned} &\mu_t = \rho \alpha u_e \delta_i \gamma \\ &\gamma = (1 + 5.5(y/\delta)^6)^{-1} \\ &y \geq y_c \end{aligned}\right\} \tag{3.5}$$

where $1 - \exp(-y/A)$ is Van Driest's damping factor, which allows the representation of the laminar sublayer. A is the damping length, which according to Cebeci and Smith is given by:

$$\begin{aligned} A &= A^+ \tfrac{\mu}{\sqrt{\rho \tau_w}} \\ A^+ &= 26. \end{aligned} \tag{3.6}$$

γ is Klebanoff's intermittency factor, which accounts for the alternatively turbulent and laminar regime which occurs around the boundary layer edge. It has been established experimentally by Klebanoff [Kl1]. The crossover value y_c is obtained by requiring the continuity of μ_t.

This model has been tested extensively by its authors, and shown to perform well in the incompressible, subsonic and transonic case. Its main drawback is the necessity to first define, and then calculate, the boundary layer edge location, and the properties of the flow at that point, in order to calculate the outer eddy viscosity. This is very difficult to do numerically with a reasonable accuracy.

To overcome this difficulty, Baldwin and Lomax [Ba1] proposed an alternate outer formulation

$$\left.\begin{aligned} &\mu_t = \alpha C_{cp} \rho Y_{MAX} F_{MAX} \gamma \\ &y \geq y_c \end{aligned}\right\} \tag{3.7}$$

where

$$F(y) = y|\omega|(1 - \exp(-\frac{y}{A})) \tag{3.8}$$

and F_{MAX} is the maximum of F in a profile, and Y_{MAX} the value of y at which it takes place. They take

$$\delta = \frac{Y_{MAX}}{C_{KL}} \tag{3.9}$$

where C_{cp} and C_{KL} are constants determined by (3.9) and (3.10):

$$C_{cp}Y_{MAX}F_{MAX} = u_e\delta_i \tag{3.10}$$

for theoretical profiles. York and Knight [Y1] have shown that, although the values $C_{cp} = 1.2$ and $C_{kl} = 0.65$ could be used for low speed flows, for high speed flows, these values depended very strongly not only on the Mach number, but also on the skin friction, making the model quite unreliable. Another difficulty of the model is that for high speeds, the function $F(y)$ does not exhibit a sharp peak as in the transonic case [Ba1], making the determination of Y_{MAX} and F_{MAX} difficult and unreliable.

As remarked before, the difficulty involved in using the Cebeci-Smith model comes from the necessity to find u_e, δ_i, and δ. We have:

$$\begin{aligned} \delta_i &= \int_0^\delta (1 - \frac{u}{u_e})dy \\ u_e\delta_i &= \int_0^\delta (u_e - u)dy. \end{aligned} \tag{3.11}$$

It is clear that an inaccurate determination of δ and $u_e = u_e(\delta)$ will result in a very inaccurate value of the eddy viscosity. However, integrating (3.11) by parts, we have:

$$u_e\delta_i = \int_0^\delta y\frac{\partial u}{\partial y}dy$$

which for an attached flow is equivalent to:

$$u_e\delta_i = \int_0^\delta y|\omega|dy \tag{3.12}$$

For high Reynolds number flows, the vorticity $|\omega|$ always decreases sharply as the distance to the wall increases, even when the boundary layer experiences pressure gradients or interaction with a shock. The function $y|\omega|$ also decreases quite quickly, as we will see in the numerical results, so that to calculate $u_e\delta_i$ using (3.12), we only need a rought estimate of δ. We obtain this estimate through the variations of the Baldwin and Lomax function F: we stop the integration in (3.12) at the point $y*$ where $F(y*)$ is lower than $F_{MAX} * \beta$, where β is an arbitrary constant. Since the function $y|\omega|$ decreases quite quickly, $\beta = 0.5$ gives an accurate enough result, and allows to separate between the boundary layer and an eventual shock.

$$u_e\delta_i = \int_0^{y*} y|\omega|dy. \tag{3.13}$$

To calculate the intermittency factor γ, we need a more accurate estimate of δ. We define a scaling length by

$$y_{av} = \frac{\int_0^{y*} y^2|\omega|dy}{\int_0^{y*} y|\omega|dy}. \tag{3.14}$$

By comparison with the theoretical profiles of Sun and Childs ([Su1]), it is found that:

$$\delta = Y_{av}/C_{KL} \tag{3.15}$$

where C_{KL} is a constant which depends only slightly on the flow parameters, see Fig. 7, and which can be taken to be:

$$C_{KL} = 0.45 \tag{3.16}$$

for all practical purposes.

In the original Baldwin and Lomax model, the damping length A was calculated using only wall quantities.

$$A = A^+ \frac{\mu_w}{\sqrt{\rho_w \tau_w}}.$$

There is no significant difference with (3.6) for low Mach numbers, because the density and molecular viscosity do not vary much, but for high speed flows, there is a difference, and Cebeci's expression (3.6) was found to give better results.

Finally, the model we are using for zero pressure gradient boundary layers is μ_t given by (3.4) in the inner layer, with the damping length given by (3.6), and in the outer layer,

$$\mu_t = \rho \alpha u_e \delta_i \gamma \tag{3.17}$$

with $u_e \delta_i$ given by (3.13), and

$$\gamma = (1 + 5.5(\frac{C_{KL} y}{y_{av}})^6)^{-1} \tag{3.18}$$

where the length scale y_{av} is given by (3.14).

Two high speed flows over flat plates were computed, and the results were compared with the experimental data of Hopkins et al. [Ho1]. Unfortunately, high speed measurements are quite scarce, and only skin friction values were available. The first case is a flow at $M_\infty = 7.4, Re\infty/m = 8 \times 10^6$. The plate has a length of 2 and a height of 0.35; the grid has 2960 nodes and 5688 elements (Fig. 8), it was generated by splitting the quadrangles of a 74×40 grid through their diagonal. The shock is captured at the leading edge. The free stream temperature is $T_\infty = 97.3K$, while the temperature at the wall is $T_w = 311K$, which is about one third of the adiabatic temperature. The molecular viscosity is given by Sutherland's law.

Figure 9 shows the pressure coefficient, skin friction and heat flux versus the streamwise coordinate x. The capturing of the shock is done sharply, as one can see from the low deviation of the pressure coefficient (less than 1%) (the leading edge is at $x = 0$). The skin friction and heat flux have the awaited behavior, starting at very high values and decreasing sharply as the Reynolds number $Re_x = Re_w \cdot x$ increases. The temperature of

the wall is lower than the adiabatic temperature, so that the heat is transferred from the flow to the wall. On Figure 10, the skin friction is plotted versus the momentum Reynolds number, and compared with the data of Hopkins et al. The agreement is very good, except for the first point, at $Re_\theta = 800$, which is in transitional flow, while no attempt to account for the transition has been made here. The streamwise variations of $\theta, u_e \times \delta_i$ and Y_{av} are also presented. It can be seen that they are very smooth, although a few discontinuities appear near the end of the plate, where the higher and coarser part of the grid plays a role. The crosswind profiles at $x = 1.45$ of the speed, the density, the turbulent and the total shear stress, and of $\omega * y$ are presented on Figure 11. Although no experimental data was available for comparison, the results are quite reasonable, at least qualitatively. The profile of density exhibits a minimum shortly of the wall; this is consistent with the fact that the wall is colder than the corresponding adiabatic wall. This peak of density induces a peak in total shear stress, because the eddy viscosity is proportional to the density. This behavior is maybe not physical, and a drawback of the mixing length theory. We have checked that it is not dependent on whether local or wall flow properties are used in the calculation of the damping length. As announced before, the function $\omega * y$ decreases quite quickly when approaching the boundary layer edge, and it can be integrated easily with a reasonable accuracy. This computation took about 10 hours of cpu on a Gould, of which only about 3% was due to the evaluation of the eddy viscosity. The main over cost when compared to laminar calculations comes from the slower convergence to steady state: the resolution algorithm is a linearly implicit pseudo-time marching to steady state, in which the variations of the eddy viscosity with respect to time are not taken in account: at time level n, the viscosity is frozen, and the algorithm is advanced of one time step, giving the flow properties at time $n + 1$, at which the eddy viscosity is re-evaluated. This still allowed the use of a Courant number of 50 without encountering stability problems, but the number of iterations necessary to converge to steady state was about 50% more than in the laminar case, giving a 50% overcost.

Another of the test cases of Hopkins et al., at a higher wall temperature, was computed. The geometry is the same as previously; the Mach number is $M_\infty = 7.4$, the Reynolds number is $Re_\infty/m = 3 \times 10^7$, the free stream temperature is $T_\infty = 58K$, the wall temperature is $T_w = 305K$. The grid used has 1170 nodes and 2204 elements; it was obtained by splitting in triangles a 30×39 grid. In Figures 12, 13, and 14, the same results as for the previous case are presented. Because of the much coarser streamwise discretization, the results are less smooth, and the agreement with experimental data is not as good as for the previous case. Nevertheless, the error on the skin friction (about 8% at the maximum) is less than the estimated experimental error, so that the agreement can be considered reasonable.

IV. ALGEBRAIC MODELS FOR HIGH SPEED SEPARATED FLOWS

It is well-known that, when the boundary layer becomes separated, both the Cebeci-Smith and the Baldwin-Lomax model give erroneous results, because they rely on Prandtl's mixing length theory, which is no longer relevant. This has been observed by many authors (see e.g., [V1], [Y1]), and is maybe the major drawback of these models. Some improvement can be obtained by using the Cebeci-Smith model, and modifying the Van Driest damping factor ([V1]), but the results are still not very good in and downstream of the separated zone.

In 1986, Goldberg ([Go1]) proposed a new algebraic $k-\varepsilon$ model to account for separated regions. His model is based on the following assumptions and observations on the separated region: the stress scale is given by the maximum shear stress in the separated layer, not by the wall stress; the shear layer has qualitatively the same turbulent structure when it is detached as when it is attached, and the length scale is the height of the separated region. Considering this, and continuity arguments, he proposed to take the kinetic energy of turbulence to be

$$k = k_b \frac{1 - \exp(-\phi(\frac{y}{y_b})^2)}{1 - \exp(-\phi)} \tag{4.1}$$

where the subscript b refers to the backflow edge (defined by the point where the tangential speed is zero), and where ϕ is a parameter, found empirically to be $\phi = 0.5$.

The turbulence energy dissipation is taken to be

$$\varepsilon = \frac{k^{\frac{3}{2}}}{y_b} \tag{4.2}$$

because the length scale is y_b.

For high Reynolds number flows, k_b can be taken to be, by analogy with the attached case,

$$k_b = \frac{u_s}{\sqrt{C^*}} \tag{4.3}$$

where $C^* = 0.09$, and where

$$u_s = \sqrt{-(u'v')_{\max}}$$

if $\overline{-(u'v')}_{max}$ is the maximum turbulent shear stress, which occurs in the detached layer, and must be provided by the model used outside the separation bubble.

Altogether, the kinematic eddy viscosity is taken as

$$\begin{aligned} \nu_t &= f(y)(\tfrac{k^2}{\varepsilon})\sqrt{\tfrac{\rho_w}{\rho}} \\ &= C_1 u_s y_b \sqrt{\tfrac{\rho_w}{\rho}} f(y)\sqrt{G(y)} \end{aligned} \tag{4.4}$$

where

$$f(y) = A\frac{y}{y_b} + B \tag{4.5}$$

The function f accounts for the laminar part in the vicinity of the wall, the constant A and B are found to be optimal at

$$A = -\left(\frac{C_\mu^*}{2}\right)^{\frac{2}{5}}$$

$$B = \left(\frac{C_\mu^*}{2}\right)^{\frac{3}{5}} - A$$

$$C_\mu^* = 0.7.$$

The function G is the Gaussian:

$$G(y) = \frac{1 - \exp(-\phi(y/y_b)^2)}{1 - \exp(-\phi)}. \tag{4.6}$$

Goldberg tested his model by computing a supersonic flow over a compression corner, and obtained impressively good results, including the correct prediction of separation and reattachment [Go1].

To take in account separation, we will use the following blend of Cebeci's and Goldberg's models. In the attached regions, we use the Cebeci model as described before, only replacing in the van Driest damping factor the wall shear stress by the maximum shear stress in the profile, to avoid an unphysical reduction of the eddy viscosity near separation and reattachment.

For separated profiles, consistently with Goldberg's hypothesis, we suppose that the shear layer is not qualitatively disturbed by the separation, so that we can take the eddy viscosity in it to be given by the Cebeci model, provided we use the distance to the backflow edge instead of the distance to the wall. In other words, μ_t is given by

$$\left.\begin{aligned} \mu_t &= \rho\ell^2|\omega| \\ \ell &= x(y - y_b)\left(1 - \exp\left(-\tfrac{y-y_b}{A}\right)\right) \end{aligned}\right\} \tag{4.7}$$

for $y_b \leq y \leq y_c$ and

$$\mu_t = \alpha u_e \delta_i \left(1 + 5.5\left(C_{KL}\frac{y - y_b}{y_{av}}\right)^6\right)^{-1} \tag{4.8}$$

for $y \geq y_c$ where

$$u_e\delta_i = \int_{y_b}^{y^*} y|\omega|dy \tag{4.9}$$

$$y_{av} = \frac{\int_{y_b}^{y*} y^2|\omega|dy}{\int_{y_b}^{y*} y|\omega|dy}. \tag{4.10}$$

In the separation bubble, i.e., for $y \leq y_b$, we use Goldberg's model, as described by (4.4).

The implementation of this model is no major problem in our framework, since we have well defined normals to the wall, on which we can easily compute $y_b, y*$, and the integrals (4.9) and (4.10) giving $u_e\delta_i$ and y_{av}. The cost, in terms of cpu or storage, is not significantly different for this model as compared with the preceding one, and remains very small ($\approx$ 2% of the cpu time is used to compute the eddy viscosity).

Separation usually occurs at points where the solid wall is not convex; at these points, the influences of the two convex components on one given fluid point are taken into account, and averaged according to

$$\mu = \frac{d_2\mu_1 + d_1\mu_2}{d_1 + d_2} \tag{4.11}$$

where the subscripts 1 and 2 refer to the two convex components of the wall, and where d is the normal distance to the wall.

The program automatically recognizes convexity defaults, and makes the needed averages. The parts of the eddy viscosity depending on the different convex components are computed separately, to allow vector processing; all this is completely geometry independent, assuming the solid wall is locally convex.

As a preliminary test of this model, a high speed, moderate Reynolds number flow overa a 15° compression corner was performed. The grid is shown in Fig. 15, it has 2782 nodes and 5345 elements, it was obtained by refining a cartesian grid, using an algorithm defined by Pouletty and Palmerio ([Po1],[Pa1]). The shock is captured at the leading edge, the corner is at 1.39 meters from the leading edge. The Reynolds number is $Re\infty/m = 4.95 \times 10^5$, the Mach number is $M_\infty = 5$; the free stream temperature is T_∞ = 83.6K, the temperature of the wall is T_∞ = 288K. Fig. 16 is a plot of the pressure. It can be seen that both the bow shock and the corner shock are captured neatly. On Figure 17, the pressure, skin friction and heat flux coefficients are plotted versus the streamwise coordinate (the corner is at $x = 0$). The boundary layer experiences a small separation in the vicinity of the corner, after which the skin friction quickly recovers high values, as awaited. Fig. 18 is a plot of the ratio μ_t/μ of the eddy viscosity to the molecular viscosity; it varies between 0 and 15 between the leading edge and the corner; the flow in this region is first laminar and then transitional. After the corner $\mu t/\mu$ increases quickly to values around 100, indicating a fully turbulent flow. Fig. 19, 20, and 21 are plots of the velocity vectors at the corner, after separation and near the outflow respectively. Fig. 22 shows profiles of speed, density, and total and turbulent shear stress at the corner ($x = 0$). These profiles have the awaited shape, although the discretization is maybe a bit coarse.

V. CONCLUSION

We have shown that algebraic turbulence models can be used in conjunction with unstructured grids, at no major overcost, both in terms of cpu time and storage; the program remains completely geometry independent, which is consistent with the spirit of finite elements and unstructured grids.

A practical way to use the Cebeci-Smith model has been proposed, for both attached and separated flows; in the latter case, Goldberg's modification has been used in the separated regions. The model has been shown to give accurate skin friction for high speed no pressure gradient boundary layers. A preliminary result for a separated flow is presented.

The major remaining open problem to be solved before the model can be trusted to give even coarse results on real configurations is transition. Whether an ad hoc representation by switching the model of if the predicted value of the eddy viscosity is lower than a critical value, as suggested by Baldwin and Lomax [Ba1], would give a relevant result, has not been investigated. More experimental data on transitional and/or separated high speed flows is certainly necessary before answers can be given.

References

[Ba1] B. S. Baldwin and H. Lomax, "Thin layer approximation and Algebraic model for separated turbulent flows," AIAA 78-257, Huntsville, January 16-18, 1978.

[Ca] G. V. Candler and R. W. MacCormack, "Hypersonic flow past 3D configurations," AIAA 87-0480, Reno, January 12-16, 1987.

[Ce1] T. Cebeci and A. Smith, "Analysis of turbulent boundary layers," Academic Press, 1974.

[Ch1] S. Chakravarthy, "High resolution upwind formulations for the Navier-Stokes equations," Von Karman Institute Lecture Series, 1988-05, March 7-11, 1988.

[Da1] F. el Dabaghi, Thesis, Universite Paris XIII, 1984.

[Go1] U. C. Goldberg, "Separated flow treatment with a new turbulence model," AIAA J., Vol. 24, No. 10, October 1986, pp. 1711-1713.

[Ho1] E. J. Hopkins, E. R. Keener, T. E. Poleh, and H. A. Dwyer, "Hypersonic turbulent skin-friction and boundary layer profiles on nonadiabatic flat plates," AIAA J., Vol. 10, No. 1, January 1972.

[J1] A. Jameson and H. Rieger, "Solution of steady three dimensional compressible Euler and Navier-Stokes equations by an implicit LU scheme," AIAA 88-0619, Reno, 1988.

[Kl1] P. S. Klebanoff, "Characteristics of turbulence in a boundary layer with zero pressure gradient," NACA TN 3178 (1954).

[Ma1] M. Mallet, J. Periaux, P. Perrier, and B. Stoufflet, "Flow modelization and computational methodologies for the aerothermal design of hypersonic vehicles: Application to the European Hermes," AIAA 88-2628, June 1988, San Antonio.

[Os1] S. Osher and S. Chakravarthy, "Upwind difference schemes for the hyperbolic systems of conservation laws," Math. Comp., April 1982.

[Pa1] B. Palmerio, "Self adaptive FEM algorithms for the Euler equations," INRIA Report 338, 1985.

[Po1] C. Pouletty, "Generation et optimisation de Maillages en elements finis, application à la résolution des équations de la mécanique des fluides," Thèse de Docteur Ingenieur, Ecole Centrale, December 1985.

[Ro1] P. Rostand and B. Stoufflet, "TVD schemes to compute compressible viscous flows on unstructured meshes," Proceedings of the 2nd International Conference on Hyperbolic Problems, Aachen (FRG), 1988 (Vieweg).

[Sh1] J. Shang and W. L. Hankey, "Numerical solution of supersonic turbulent flow over a compression ramp," AIAA J., Vol. 13, October 1975, pp. 1368-1374.

[Sp1] C. G. Speziale, "On nonlinear K-ℓ and K-ε models of turbulence," J. Fluid Mech., Vol. 178, 1987, pp. 459-475.

[St1] B. Stoufflet and L. Fezoui, "A class of implicit upwind schemes for Euler simulations with unstructured meshes," to appear in J. Comp. Phys.

[St2] B. Stoufflet, J. Periaux, L. Fezoui, and A. Dervieux, "Numerical simulations of 3D hypersonic Euler flows around space vehicles using adapted finite elements," AIAA 87-0560, Reno, January 1987.

[Su1] Sun, C. C. and M. E. Childs, "A modified wall wake velocity profile for turbulent compressible boundary layers," J. Aircraft, Vol. 10, June 1973, pp. 381-383.

[V1] M. Visbal and D. Knight, "The Baldwin-Lomax turbulence model for two-dimensional shock-wave/boundary layer interactions," AIAA J., Vol. 22, No. 7, July 1984.

[Y1] B. York and D. Knight, "Calculation of a class of two dimensional turbulent boundary layer flows using the Baldwin-Lomax model," AIAA 85-0126, Reno, January 1985.

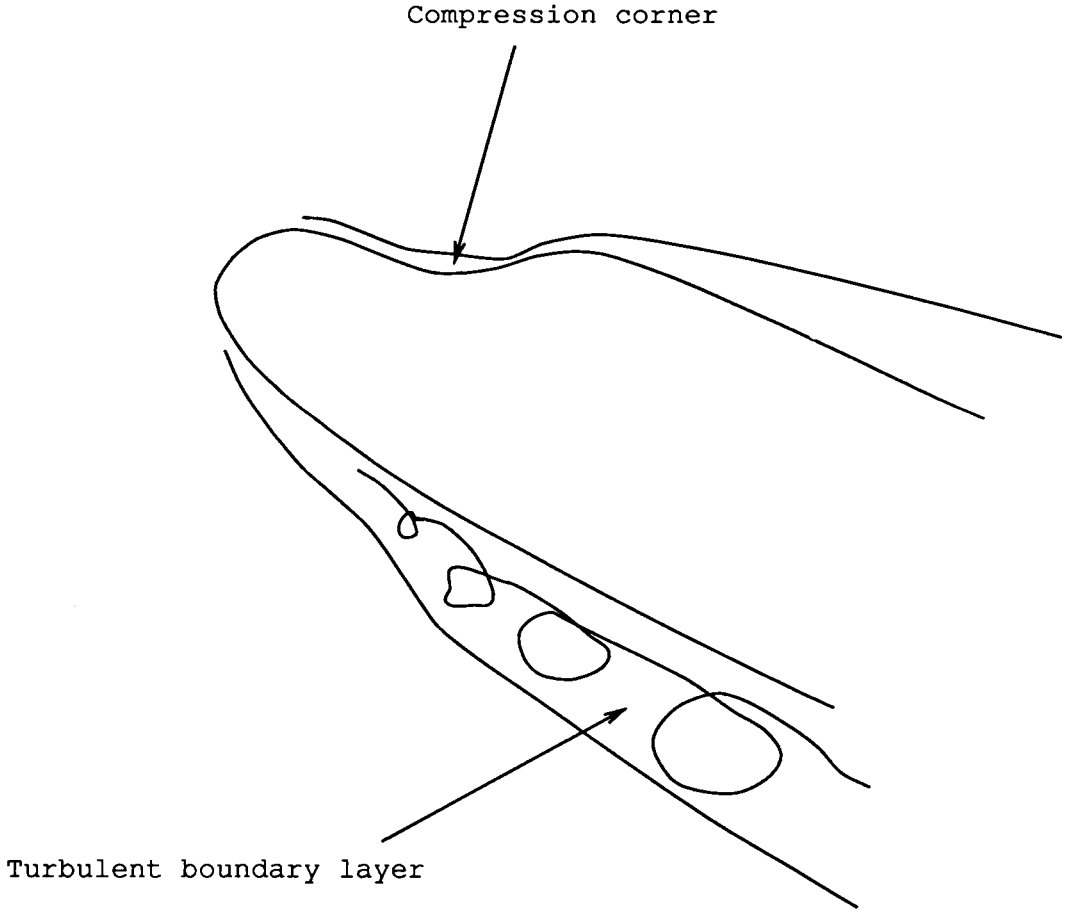

Fig. 1.

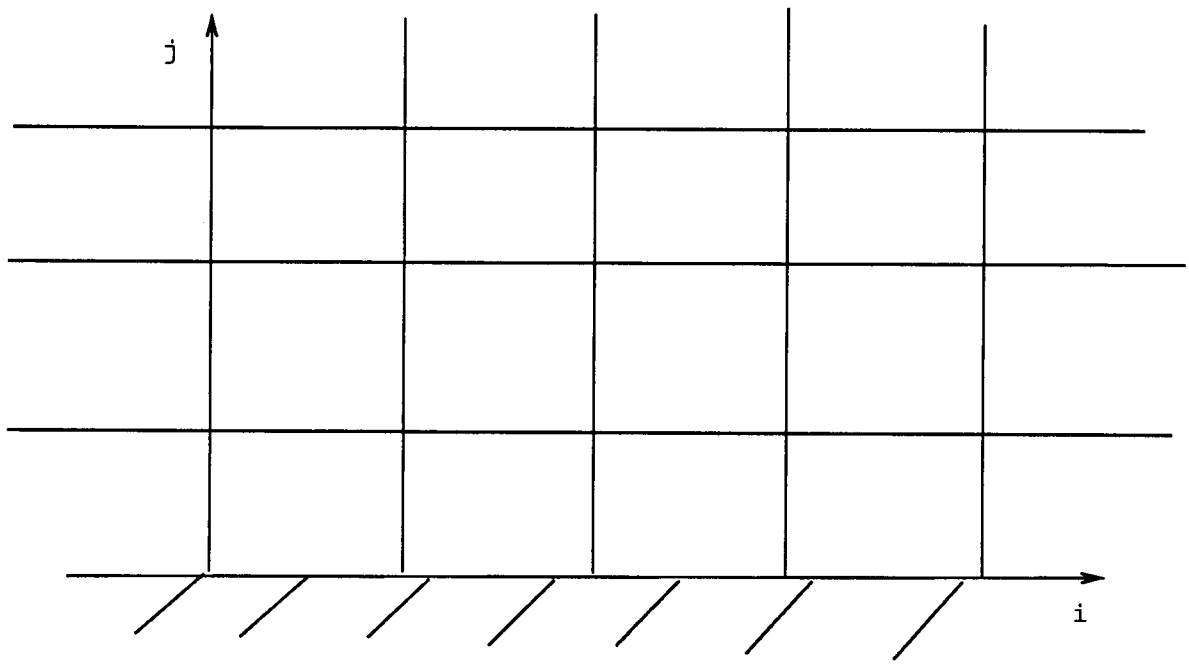

Fig. 2.

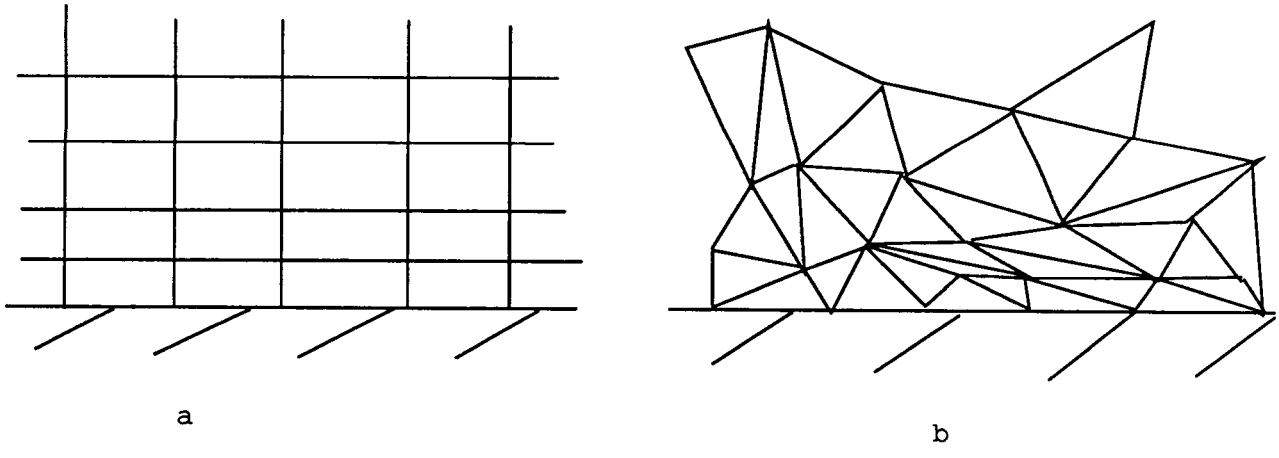

Fig. 3.

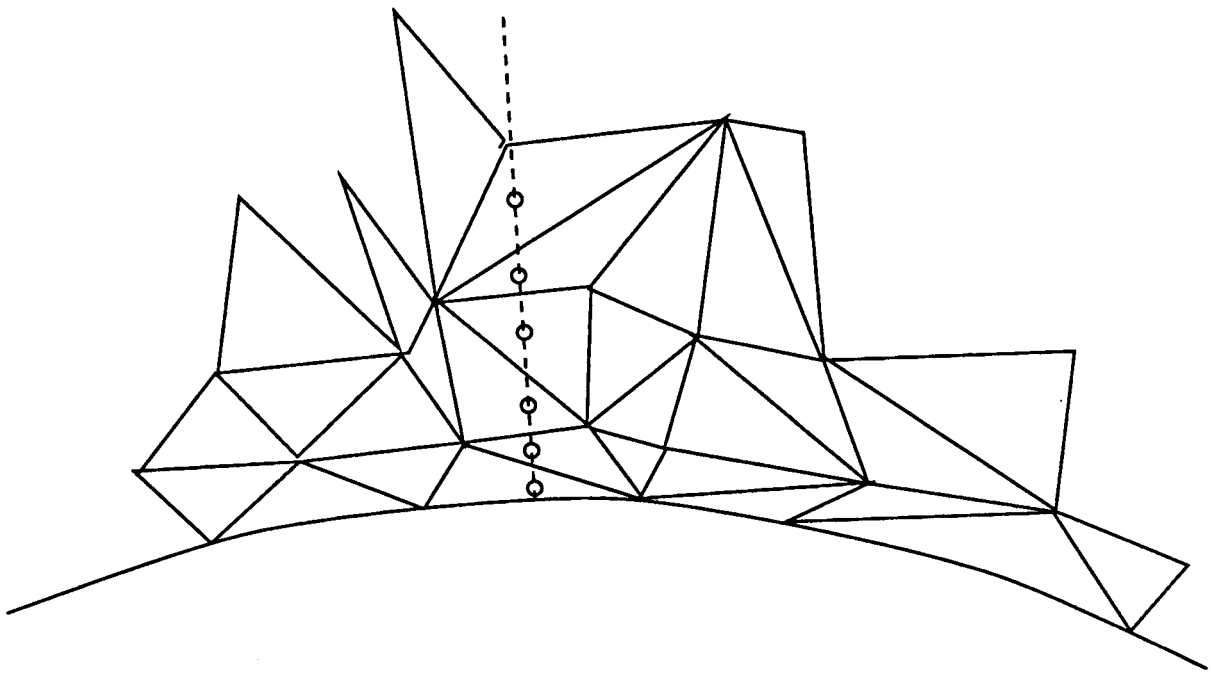

Fig. 4.

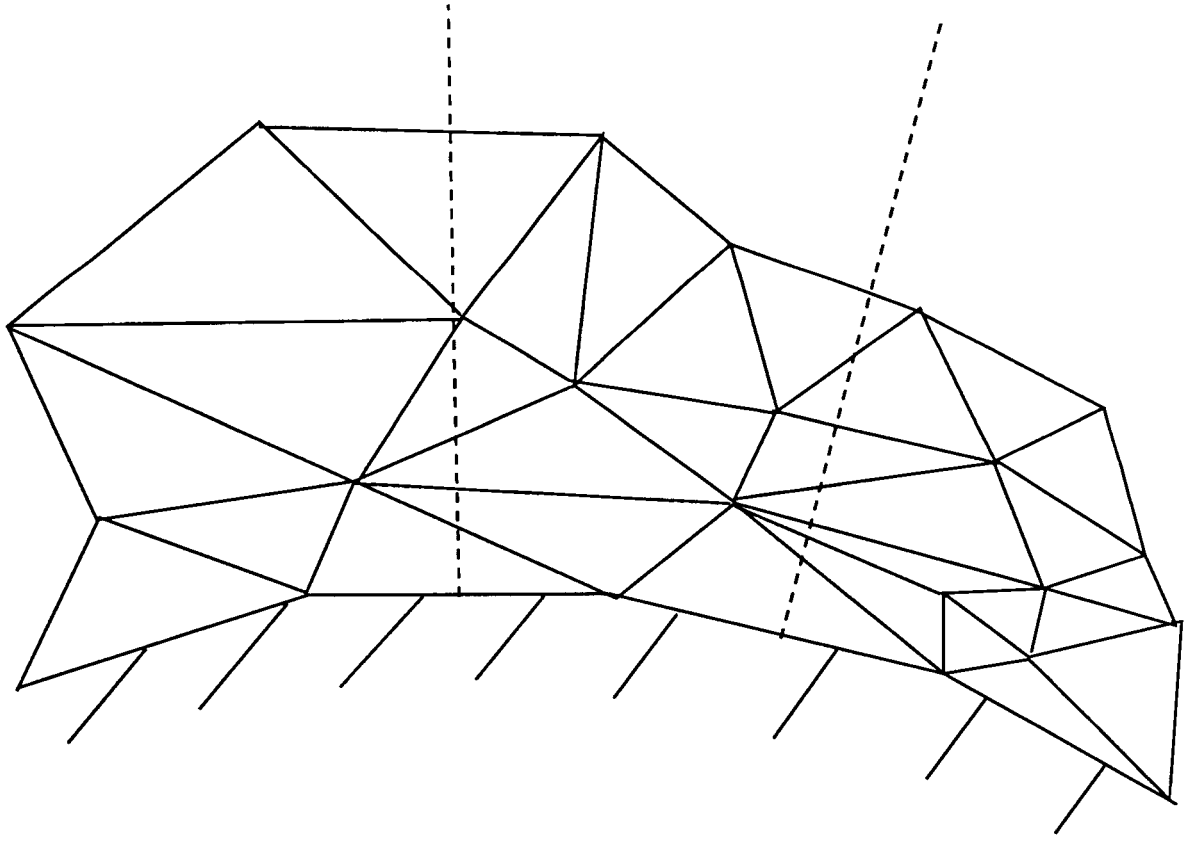

Fig. 5.

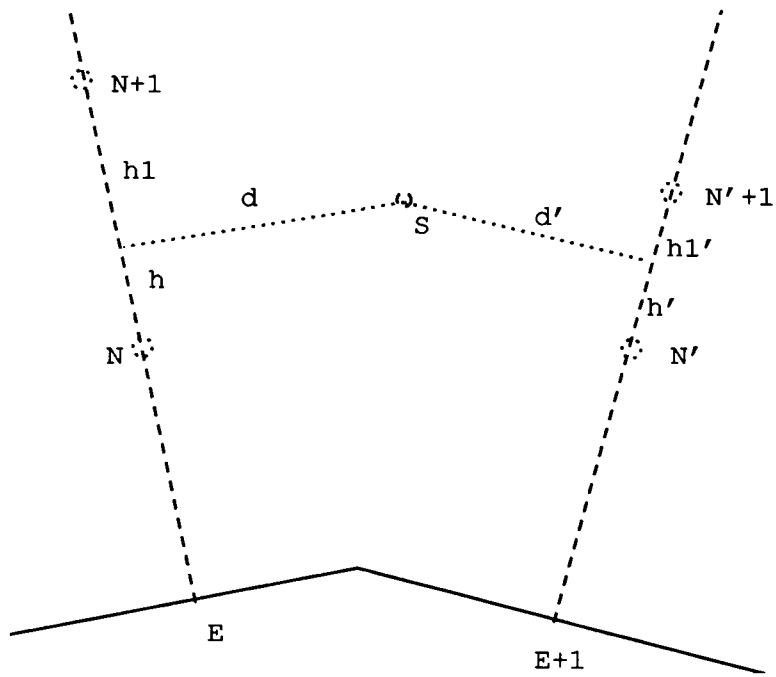

stored : E , d/(d+d') , h/(h+h1) , h'/(h'+h1')

N , N'

Fig. 6.

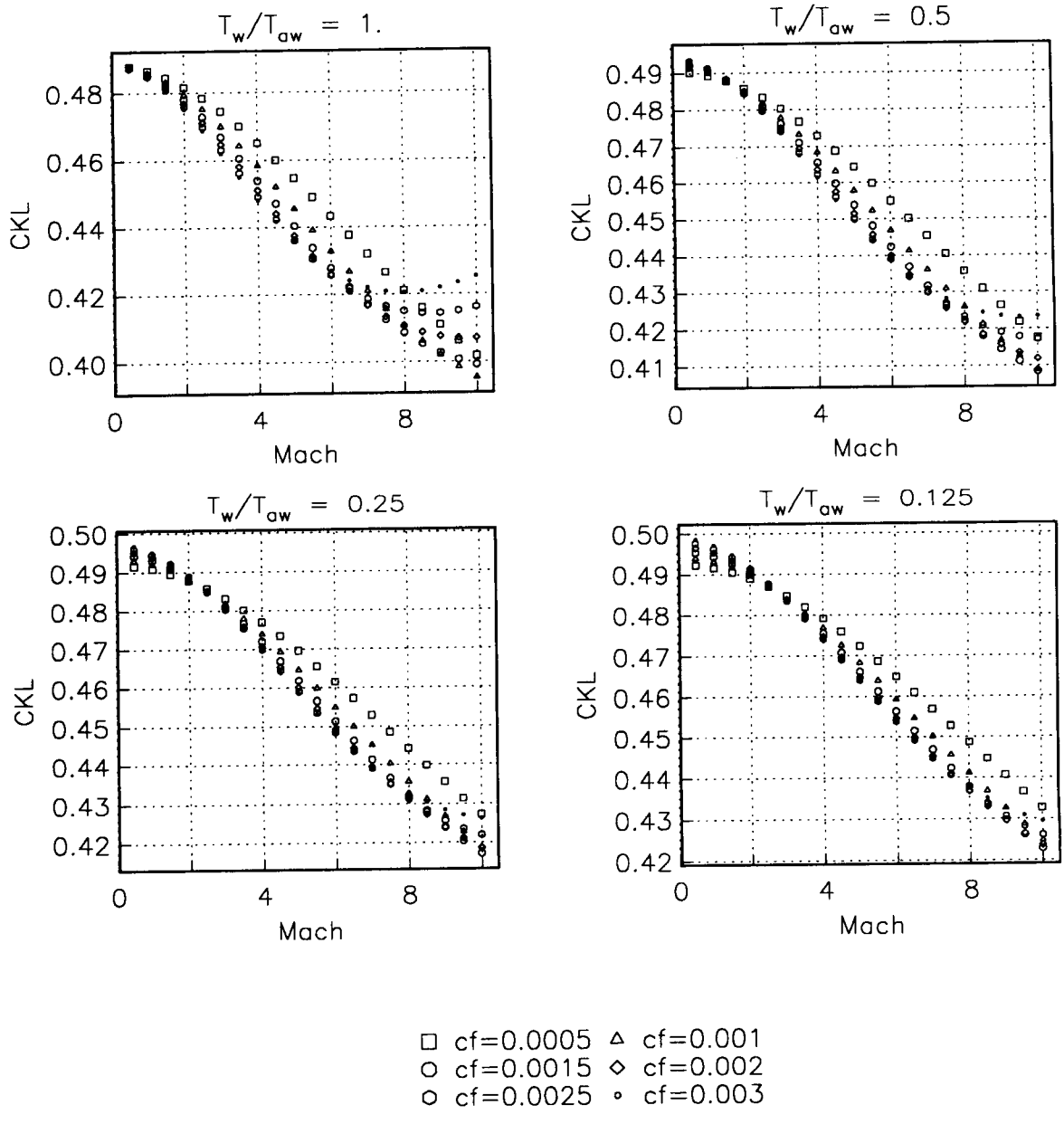

Fig. 7. Variations of C_{KL} with the flow parameters.

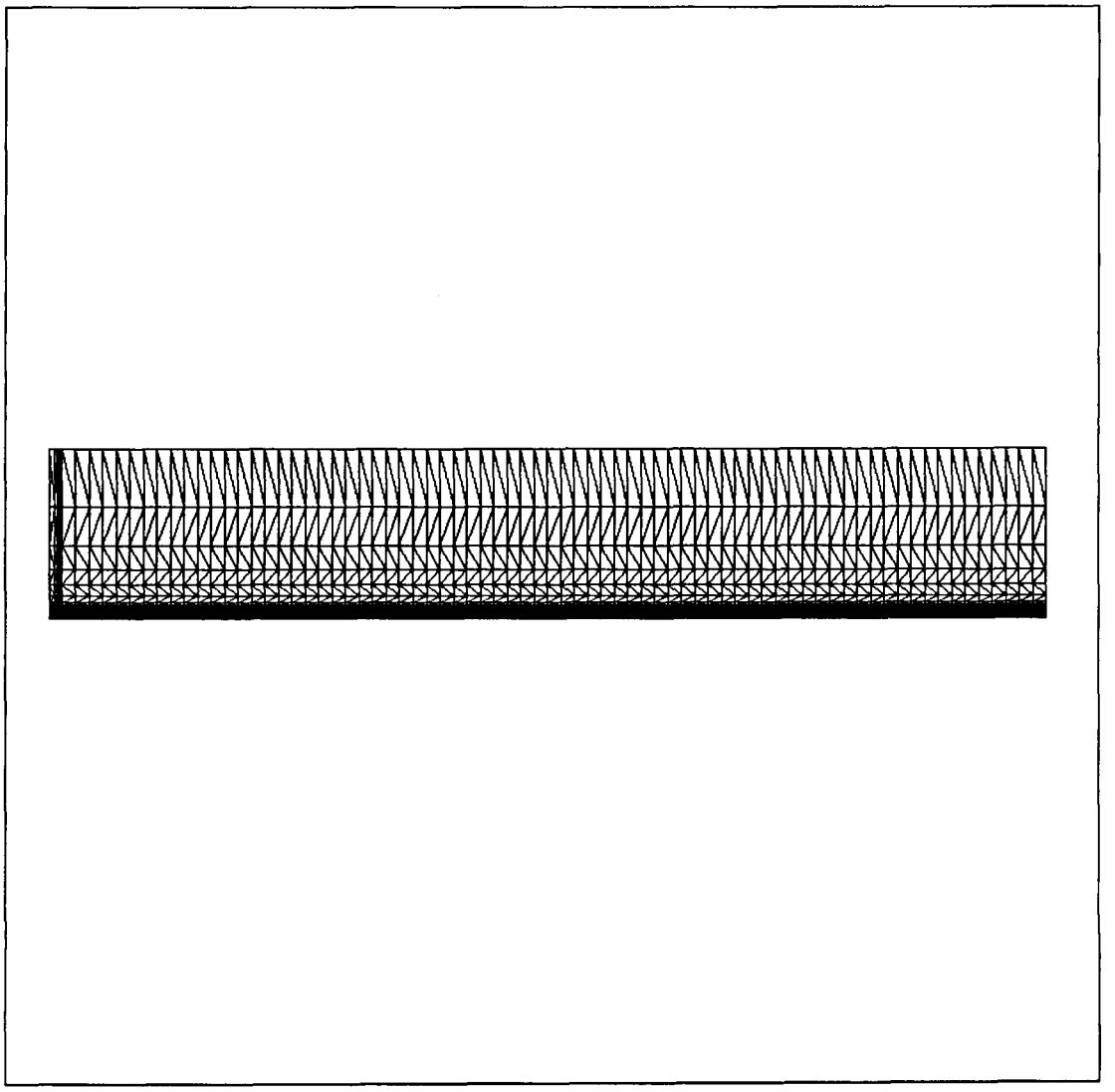

Fig. 8.

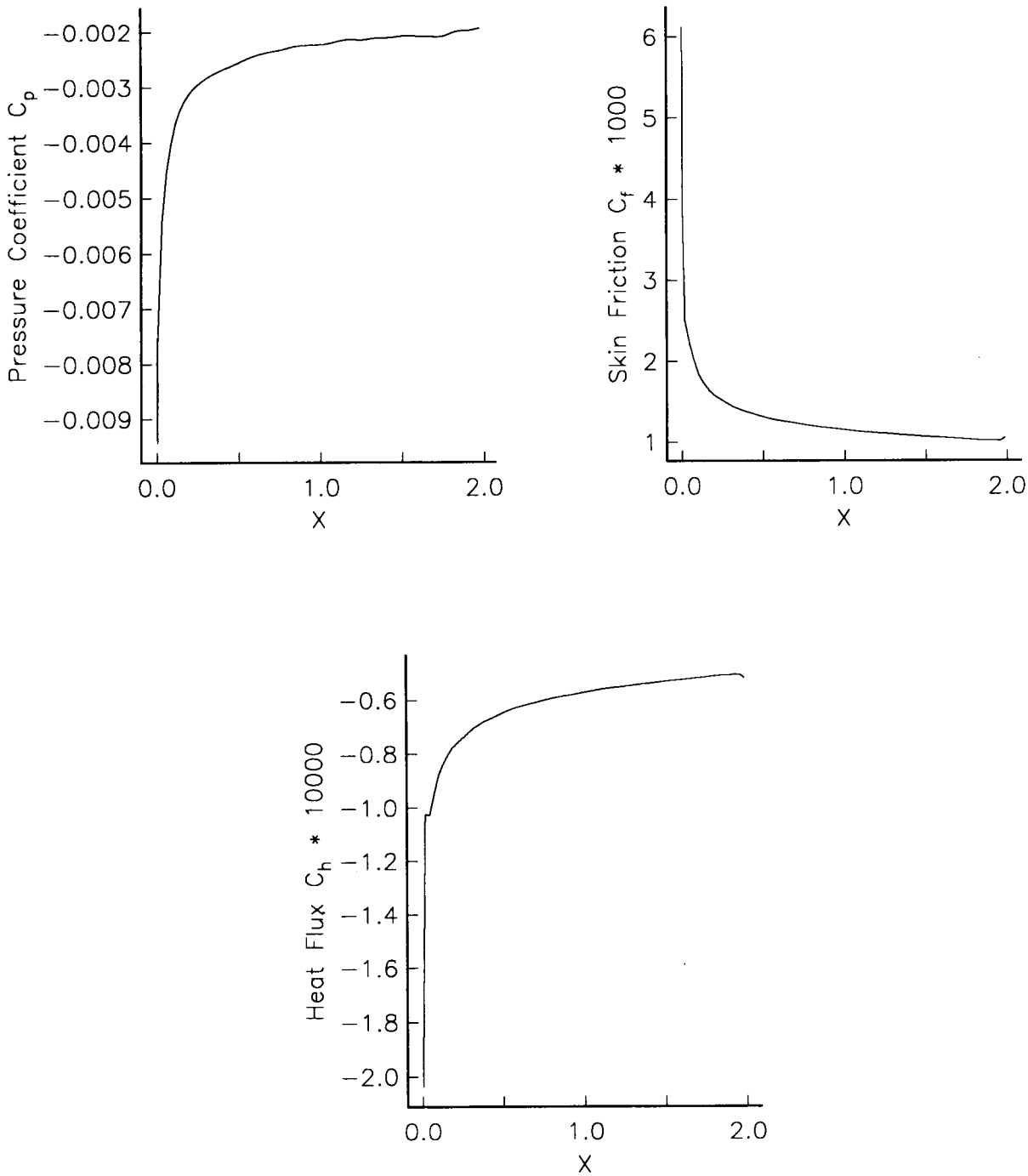
Pressure Coefficient C_p
−0.002
−0.003
−0.004
−0.005
−0.006
−0.007
−0.008
−0.009
0.0
1.0
2.0
X
Skin Friction C_f * 1000
6
5
4
3
2
1
0.0
1.0
2.0
X
Heat Flux C_h * 10000
−0.6
−0.8
−1.0
−1.2
−1.4
−1.6
−1.8
−2.0
0.0
1.0
2.0
X

Fig. 9.

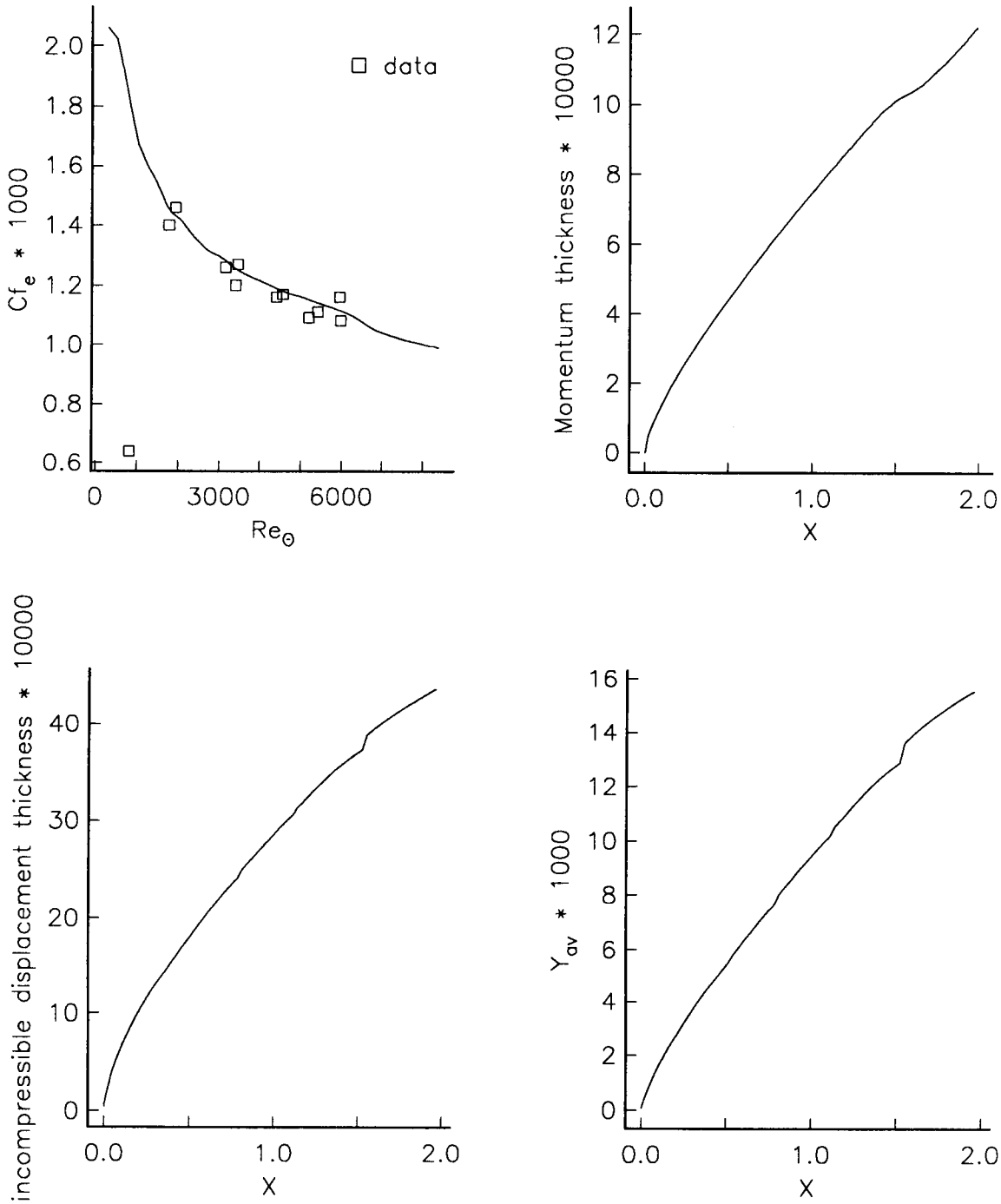
data
Cf_e * 1000
2.0
1.8
1.6
1.4
1.2
1.0
0.8
0.6
0
3000
6000
Re_Θ
Momentum thickness * 10000
12
10
8
6
4
2
0
0.0
1.0
2.0
X
incompressible displacement thickness * 10000
40
30
20
10
0
0.0
1.0
2.0
X
Y_{av} * 1000
16
14
12
10
8
6
4
2
0
0.0
1.0
2.0
X

Fig. 10.

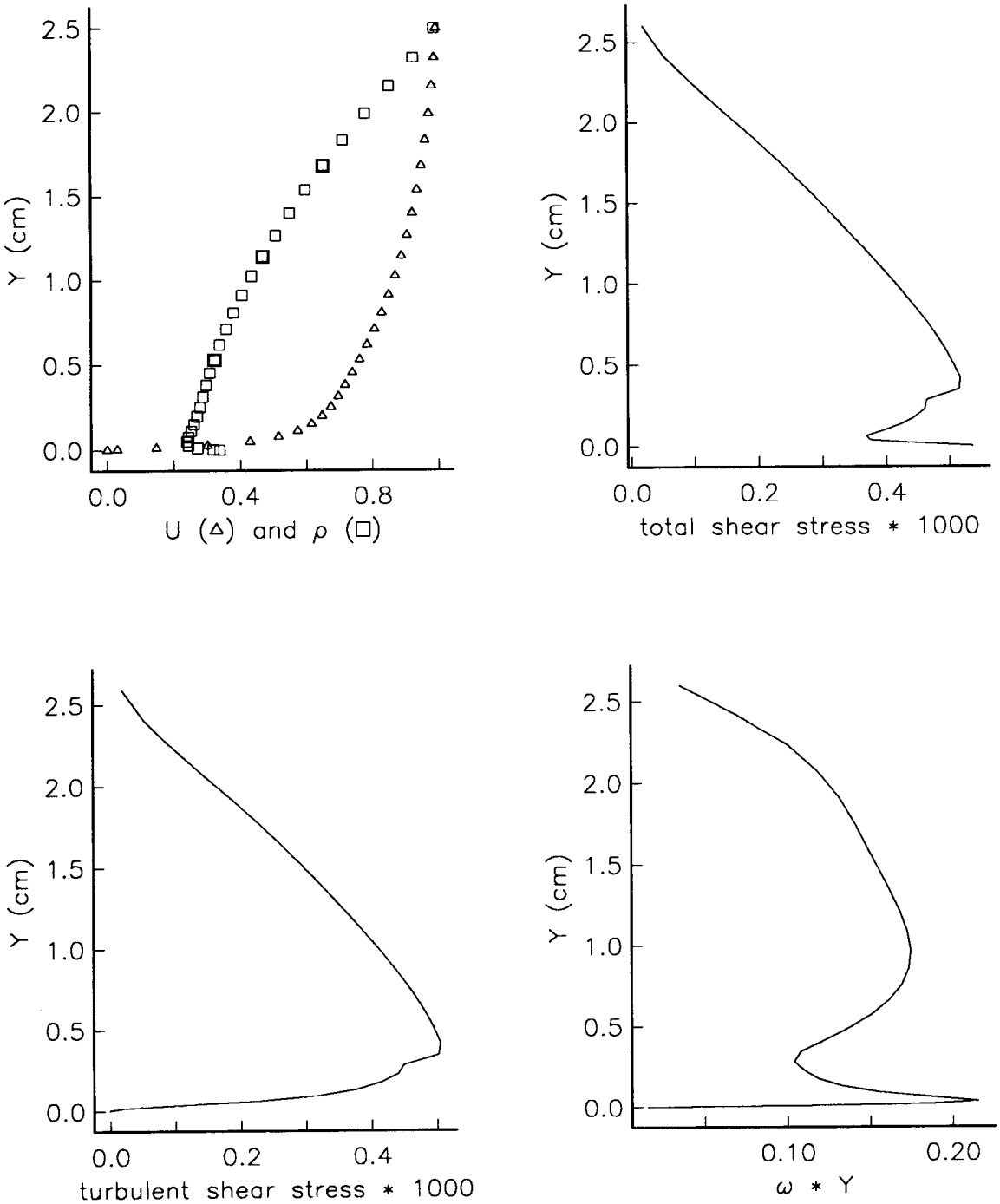
Y (cm)
2.5
2.0
1.5
1.0
0.5
0.0
0.0
0.4
0.8
U (△) and ρ (□)
0.0
0.2
0.4
total shear stress * 1000
0.0
0.2
0.4
turbulent shear stress * 1000
0.10
0.20
ω * Y

Fig. 11.

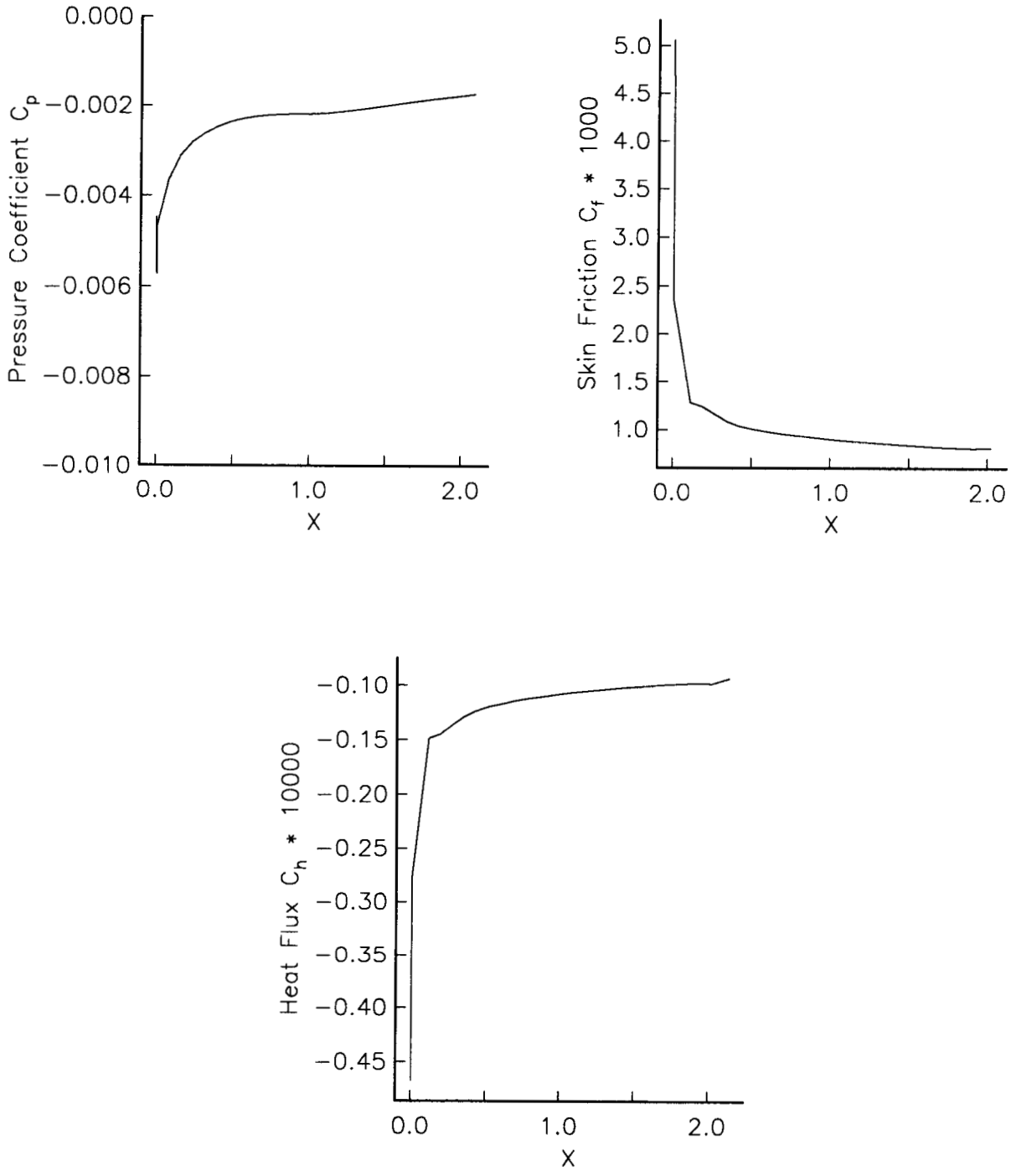
Pressure Coefficient C_p
0.000
−0.002
−0.004
−0.006
−0.008
−0.010
0.0
1.0
2.0
X
Skin Friction C_f * 1000
5.0
4.5
4.0
3.5
3.0
2.5
2.0
1.5
1.0
0.0
1.0
2.0
X
Heat Flux C_h * 10000
−0.10
−0.15
−0.20
−0.25
−0.30
−0.35
−0.40
−0.45
0.0
1.0
2.0
X

Fig. 12.

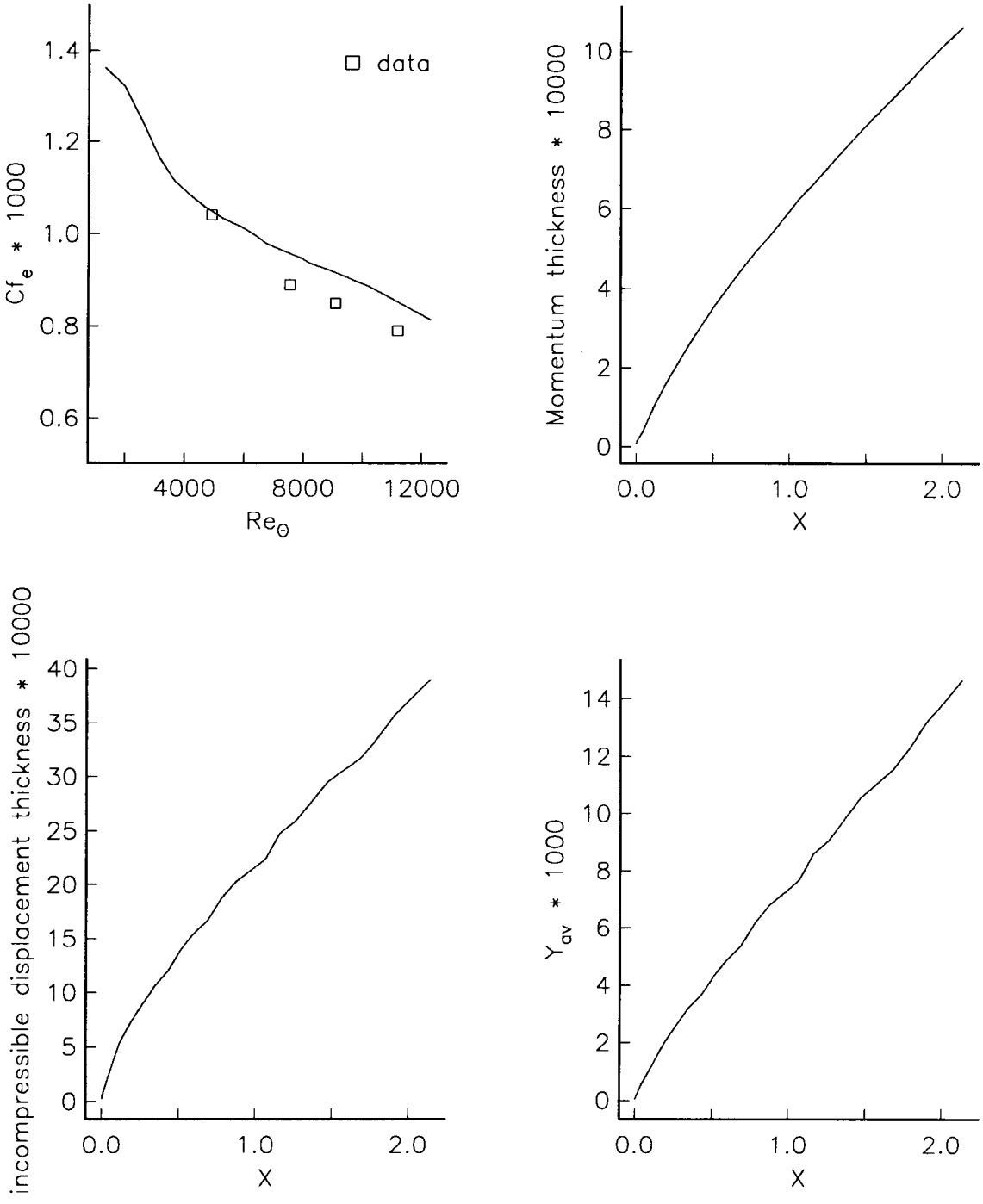
1.4
1.2
1.0
0.8
0.6
Cf_e * 1000
data
4000
8000
12000
Re_Θ
10
8
6
4
2
0
Momentum thickness * 10000
0.0
1.0
2.0
X
40
35
30
25
20
15
10
5
0
incompressible displacement thickness * 10000
0.0
1.0
2.0
X
14
12
10
8
6
4
2
0
Y_{av} * 1000
0.0
1.0
2.0
X

Fig. 13.

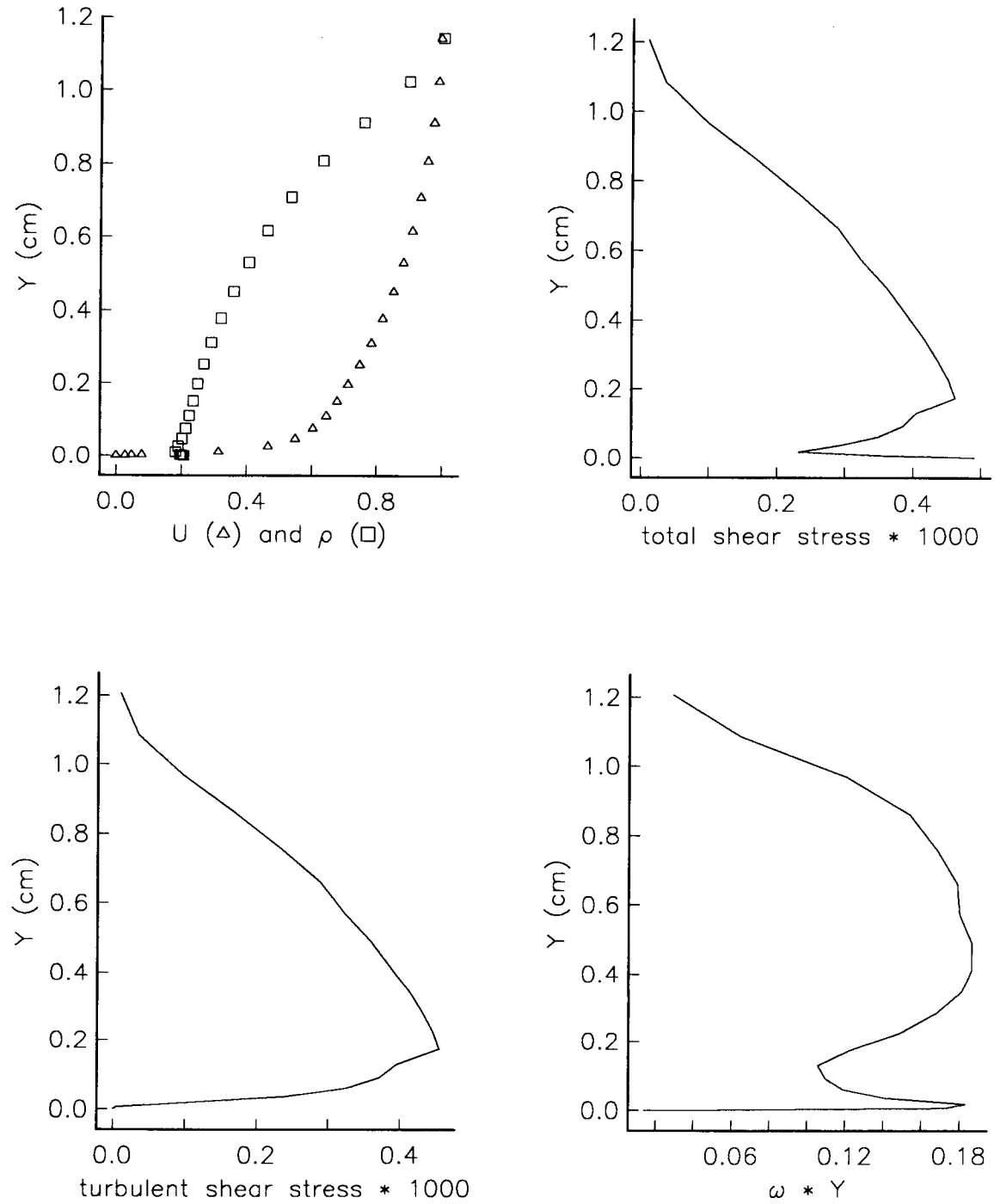
Y (cm)
1.2
1.0
0.8
0.6
0.4
0.2
0.0
0.0
0.4
0.8
U (△) and ρ (□)
0.0
0.2
0.4
total shear stress * 1000
0.0
0.2
0.4
turbulent shear stress * 1000
0.06
0.12
0.18
ω * Y

Fig. 14.

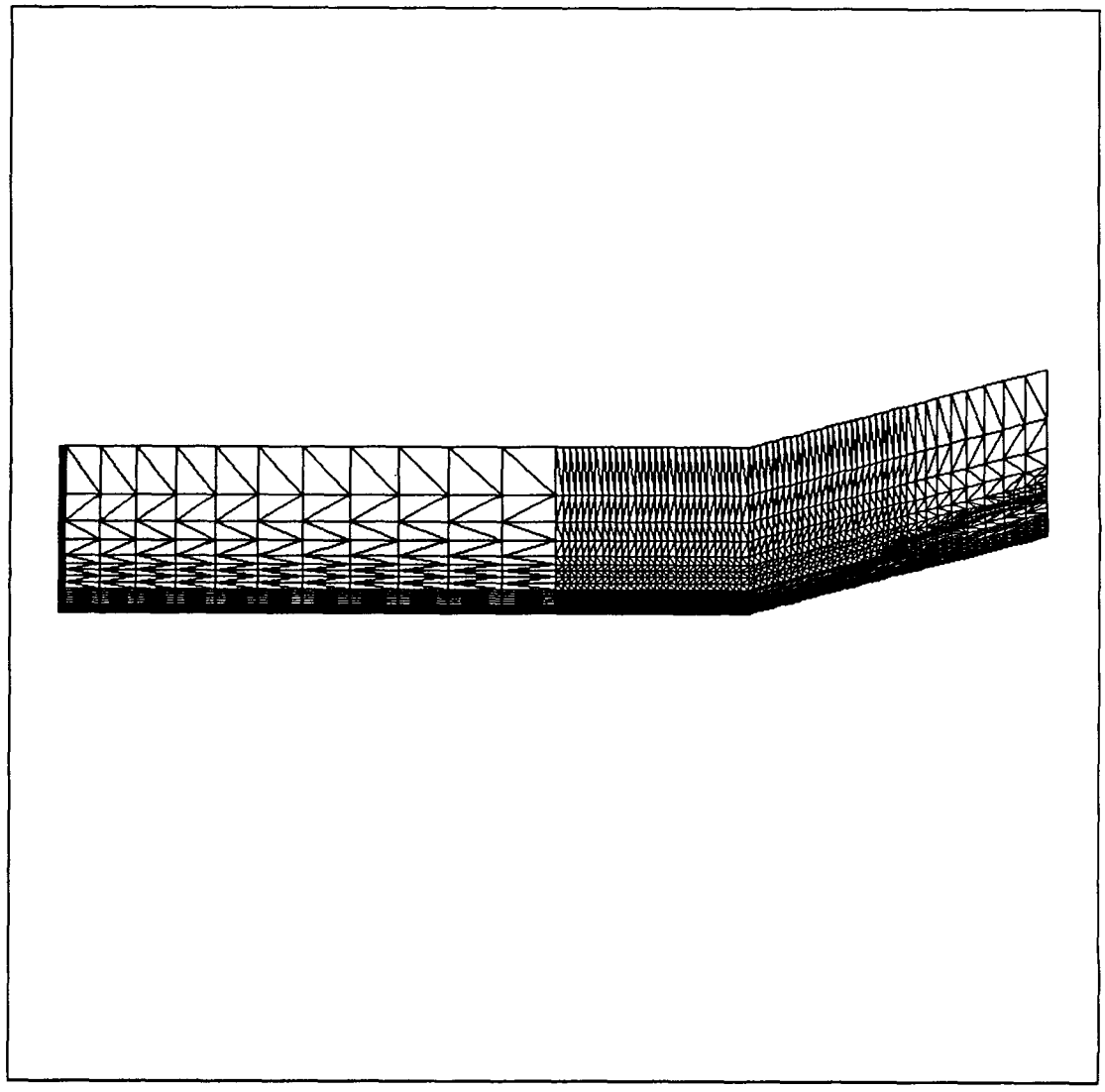

Fig. 15.

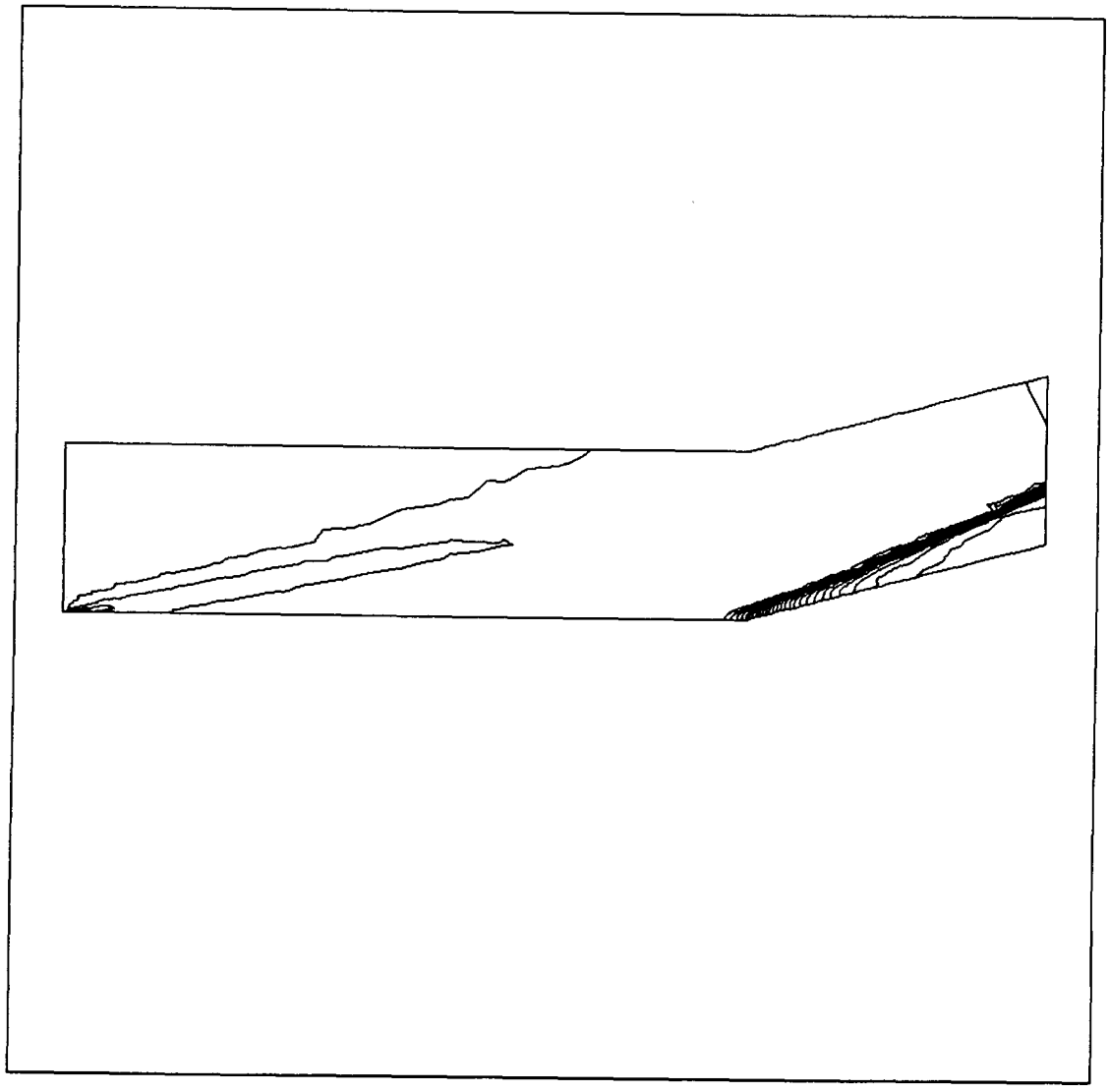

Fig. 16.

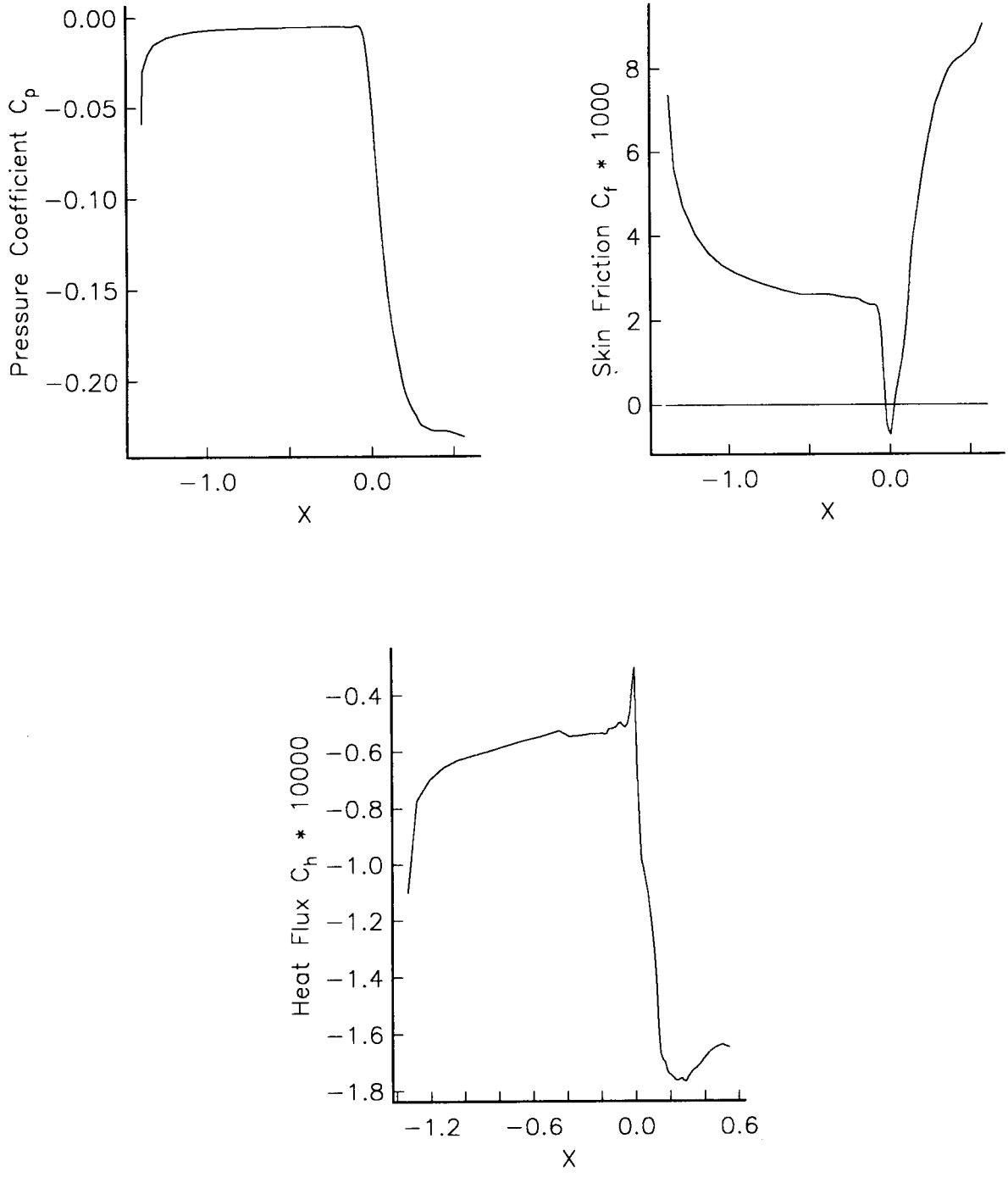
Pressure Coefficient C_p
0.00
−0.05
−0.10
−0.15
−0.20
−1.0
0.0
X
Skin Friction C_f * 1000
8
6
4
2
0
−1.0
0.0
X
Heat Flux C_h * 10000
−0.4
−0.6
−0.8
−1.0
−1.2
−1.4
−1.6
−1.8
−1.2
−0.6
0.0
0.6
X

Fig. 17.

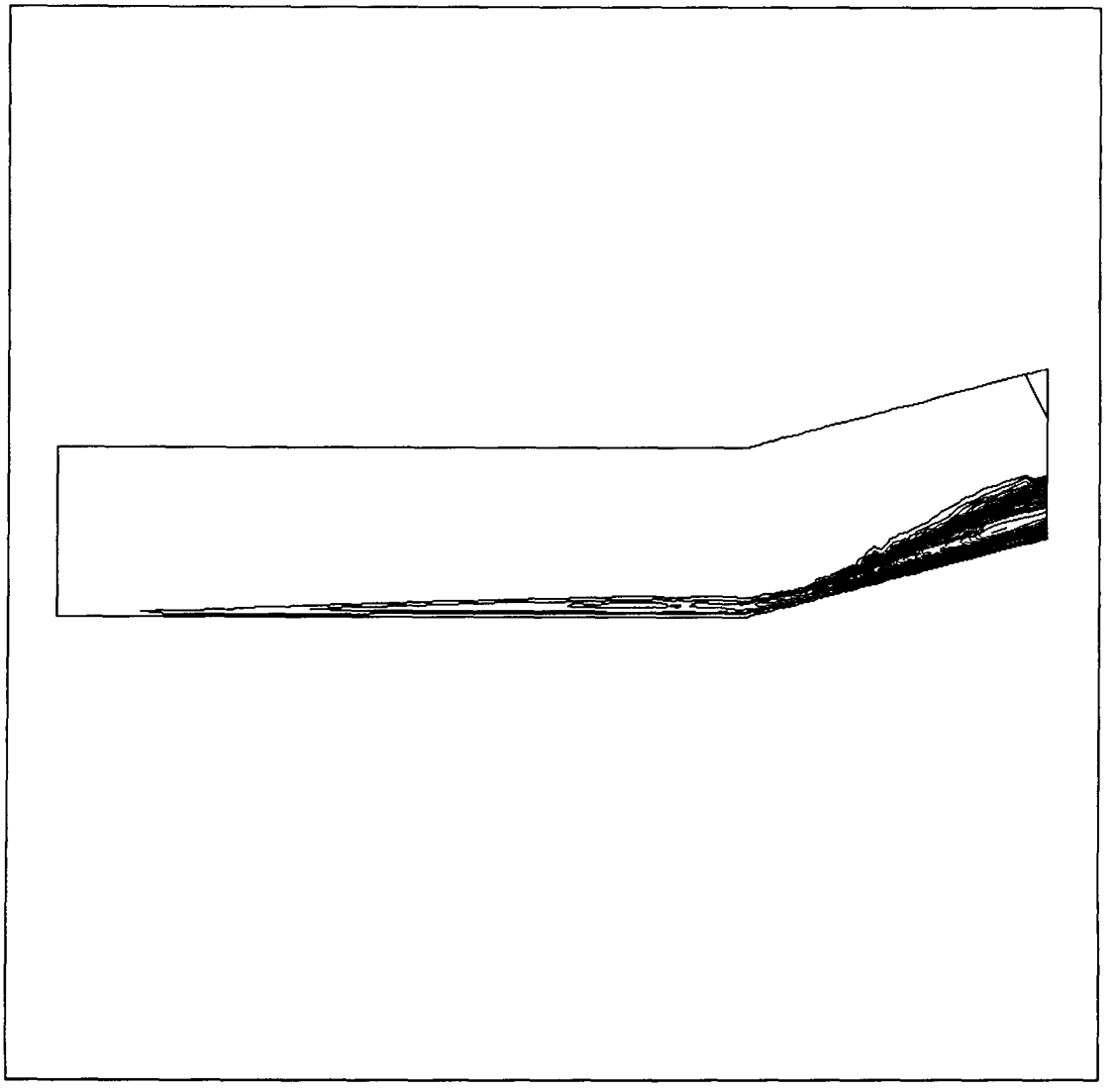

Fig. 18.

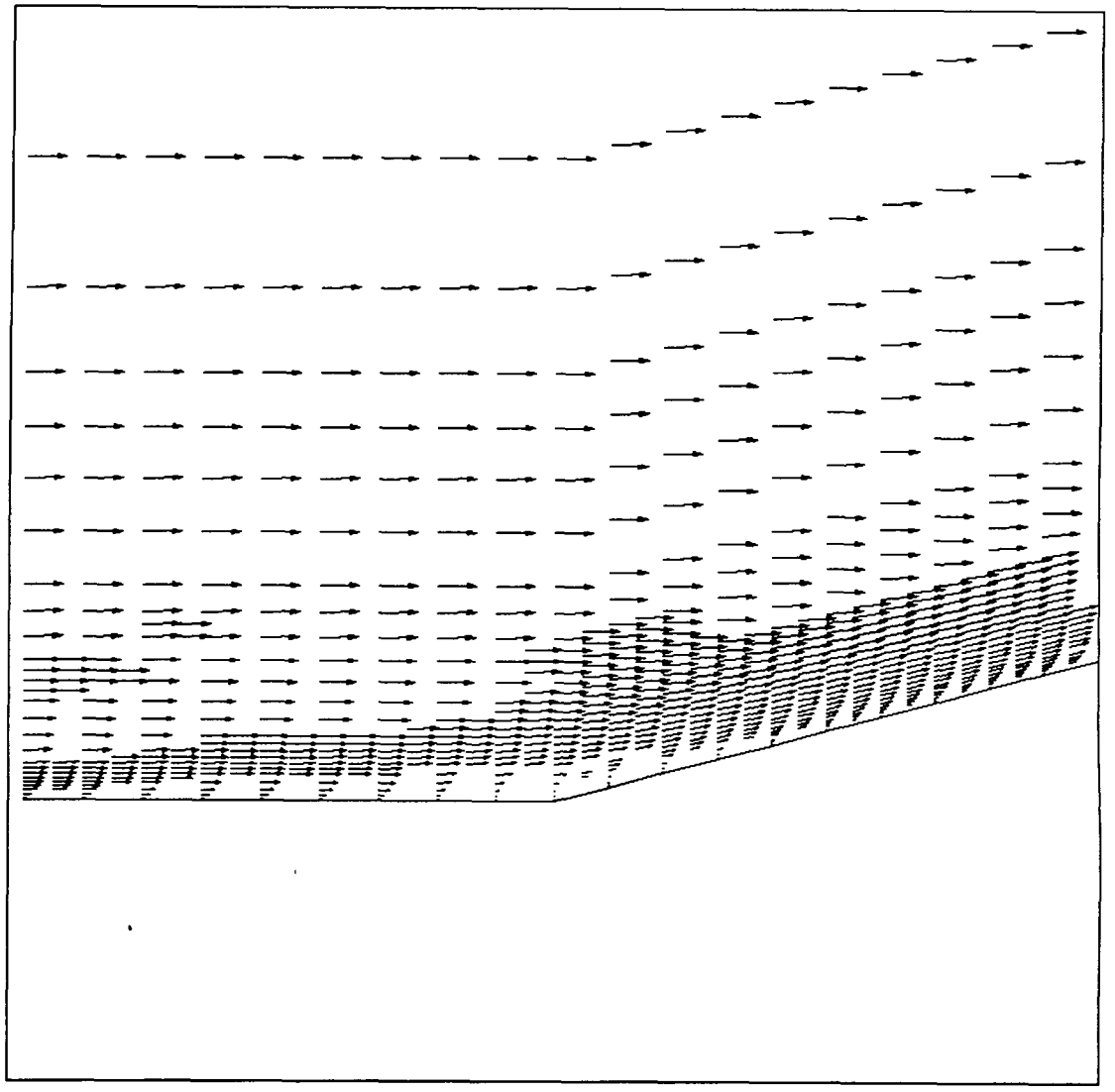

Fig. 19.

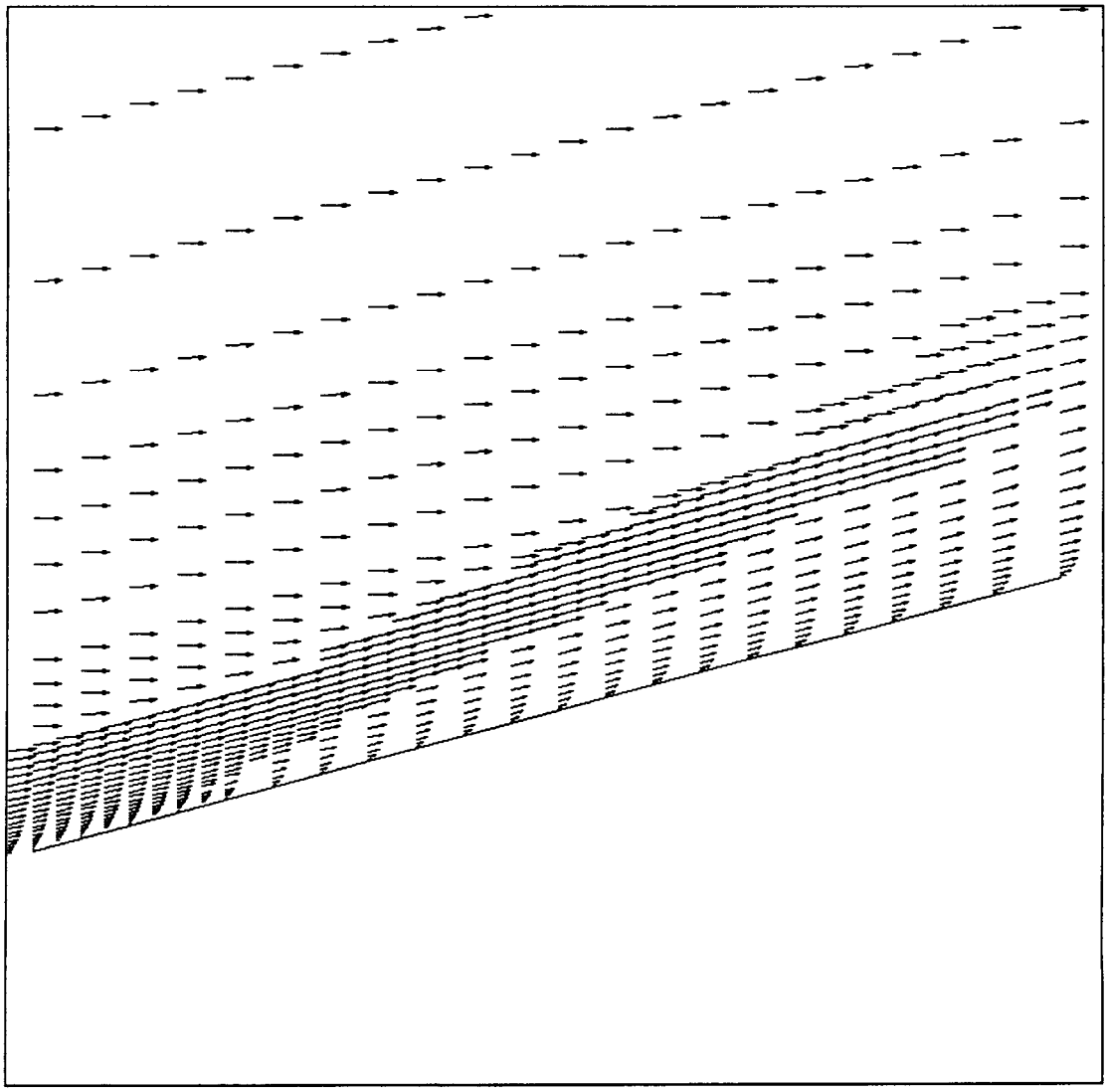

Fig. 20.

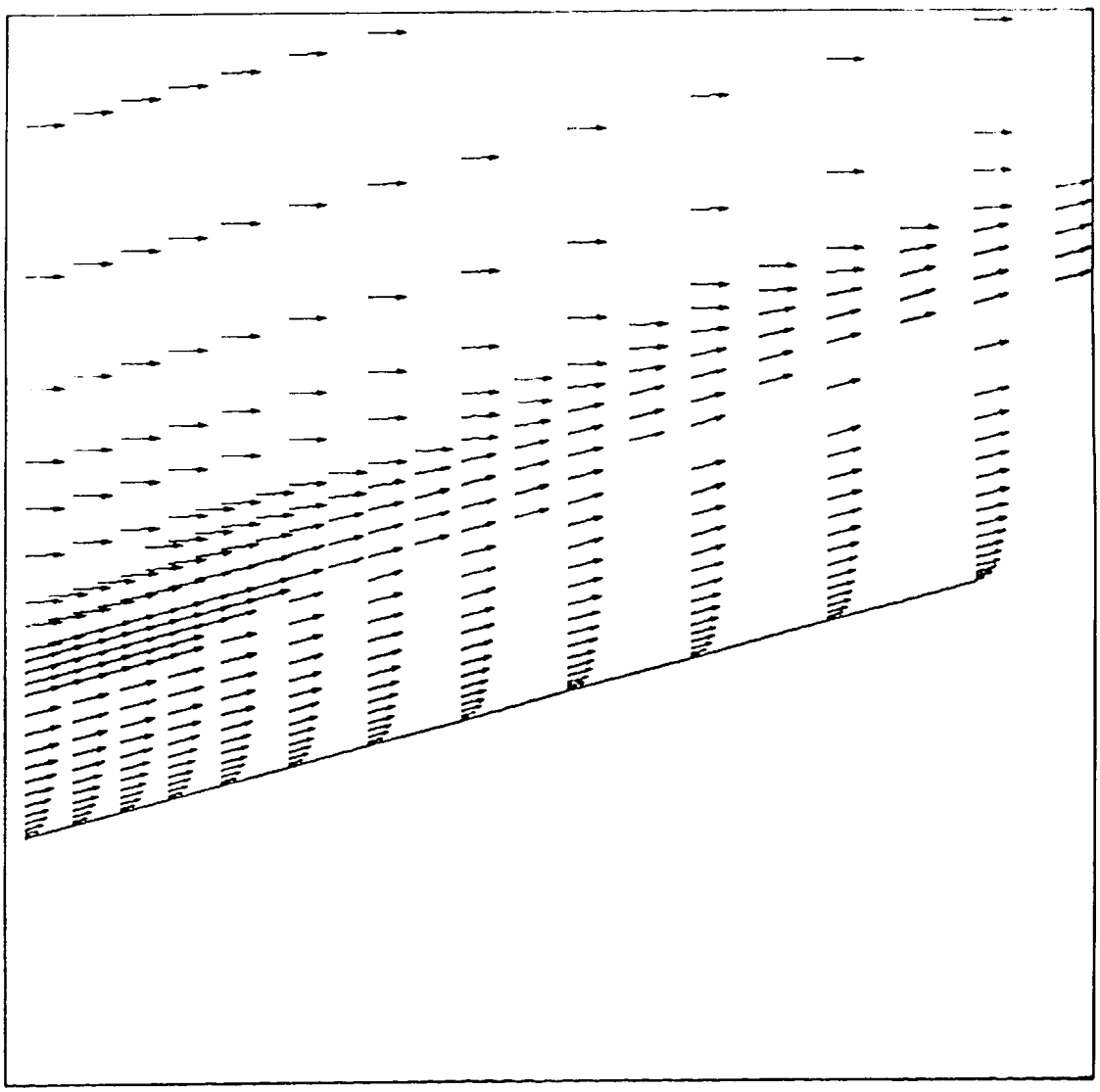

Fig. 21.

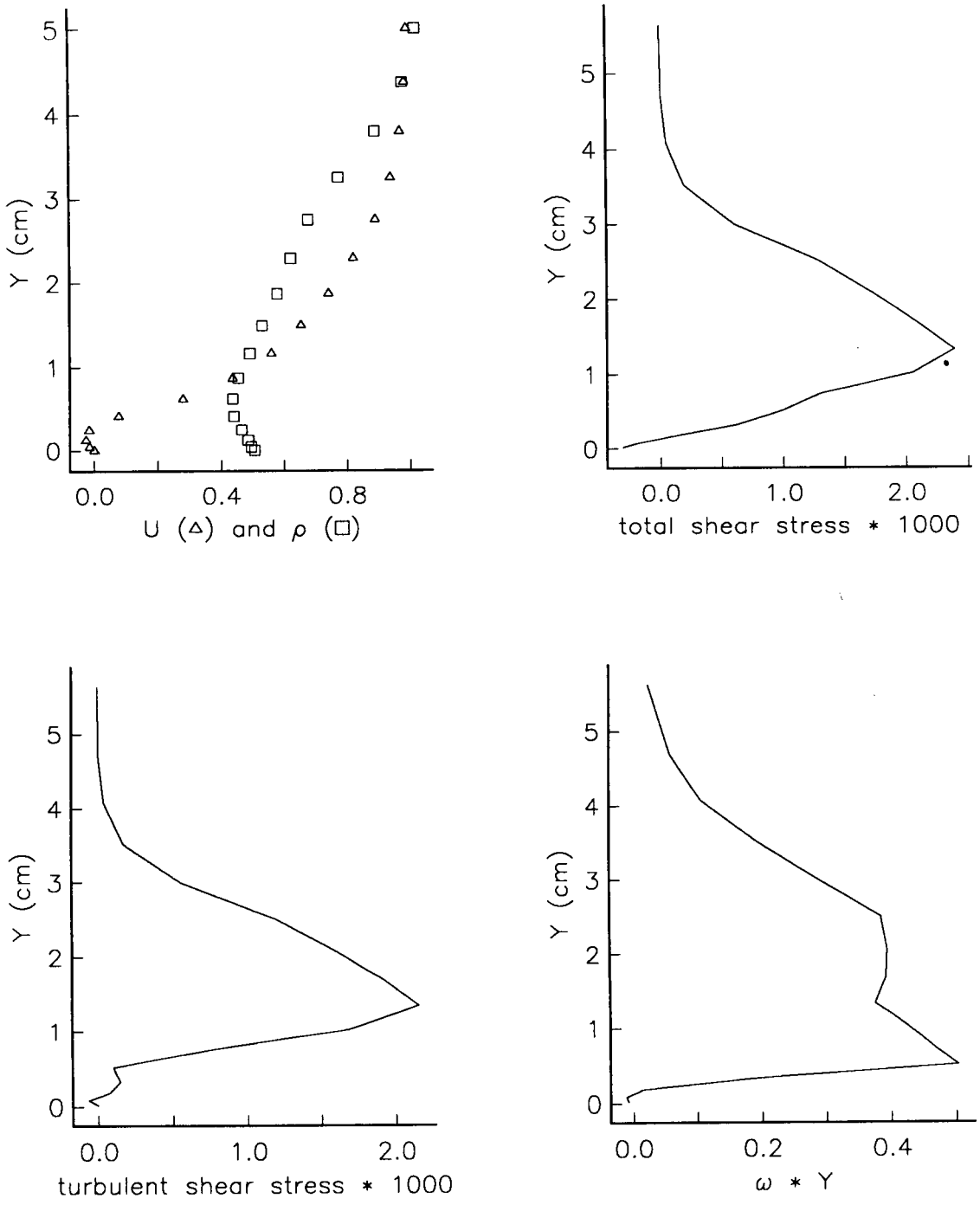
Y (cm)
0
1
2
3
4
5
0.0
0.4
0.8
U (△) and ρ (□)
0.0
1.0
2.0
total shear stress * 1000
0.0
1.0
2.0
turbulent shear stress * 1000
0.0
0.2
0.4
ω * Y

Fig. 22.

NASA National Aeronautics and Space Administration

Report Documentation Page

1. Report No.	2. Government Accession No.	3. Recipient's Catalog No.
NASA CR-181741 ICASE Report No. 88-63		

4. Title and Subtitle

ALGEBRAIC TURBULENCE MODELS FOR THE COMPUTATION OF TWO-DIMENSIONAL HIGH SPEED FLOWS USING UNSTRUCTURED GRIDS

5. Report Date

November 1988

6. Performing Organization Code

7. Author(s)

Philippe Rostand

8. Performing Organization Report No.

88-63

10. Work Unit No.

505-90-21-01

9. Performing Organization Name and Address

Institute for Computer Applications in Science and Engineering
Mail Stop 132C, NASA Langley Research Center
Hampton, VA 23665-5225

11. Contract or Grant No.

NAS1-18107, NAS1-18605

13. Type of Report and Period Covered

Contractor Report

12. Sponsoring Agency Name and Address

National Aeronautics and Space Administration
Langley Research Center
Hampton, VA 23665-5225

14. Sponsoring Agency Code

15. Supplementary Notes

Langley Technical Monitor:
Richard W. Barnwell

Final Report

Submitted to Numerical Methods in Fluids

16. Abstract

The incorporation of algebriac turbulence models in a solver for the 2D compressible Navier-Stokes equations using triangular grids is described. A practical way to use the Cebeci Smith model, and to modify it in separated regions, is proposed. The ability of the model to predict high speed, perfect gas boundary layers is investigated from a numerical point of view.

17. Key Words (Suggested by Author(s))	18. Distribution Statement
turbulence, high speed flows, triangular grids, algebraic models	34 - Fluid Mechanics and Heat Transfer 64 - Numerical Analysis Unclassified - unlimited

19. Security Classif. (of this report)	20. Security Classif. (of this page)	21. No. of pages	22. Price
Unclassified	Unclassified	43	A03